Heterogeneous Oxidation of Atmospheric Organic Aerosol: Kinetics of Changes to the Amount and Oxidation State of Particle-Phase Organic Carbon

Citation: Kroll, Jesse H., Christopher Y. Lim, Sean H. Kessler, and Kevin R. Wilson. "Heterogeneous Oxidation of Atmospheric Organic Aerosol: Kinetics of Changes to the Amount and Oxidation State of Particle-Phase Organic Carbon." The Journal of Physical Chemistry A 119, no. 44 (November 5, 2015): 10767–10783. © 2015 American Chemical Society

As Published: http://dx.doi.org/10.1021/acs.jpca.5b06946

Publisher: American Chemical Society (ACS)

Persistent URL: http://hdl.handle.net/1721.1/101649

Version: Final published version: final published article, as it appeared in a journal, conference proceedings, or other formally published context

THE JOURNAL OF PHYSICAL CHEMISTRY A

Feature Article

pubs.acs.org/JPCA

Heterogeneous Oxidation of Atmospheric Organic Aerosol: Kinetics of Changes to the Amount and Oxidation State of Particle-Phase Organic Carbon

Jesse H. Kroll,*[,†,‡] Christopher Y. Lim,[†] Sean H. Kessler,[†] and Kevin R. Wilson[§]

[†]Department of Civil and Environmental Engineering and [‡]Department of Chemical Engineering, Massachusetts Institute of Technology, Cambridge, Massachusetts 02139, United States

[§]Chemical Sciences Division, Lawrence Berkeley National Laboratory, Berkeley, California 94720, United States

ABSTRACT: Atmospheric oxidation reactions are known to affect the chemical composition of organic aerosol (OA) particles over timescales of several days, but the details of such oxidative aging reactions are poorly understood. In this study we examine the rates and products of a key class of aging reaction, the heterogeneous oxidation of particle-phase organic species by the gas-phase hydroxyl radical (OH). We compile and reanalyze a number of previous studies from our laboratories involving the oxidation of single-component organic particles. All kinetic and product data are described on a common basis, enabling a straightforward comparison among different chemical systems and experimental conditions. Oxidation chemistry is described in terms of changes to key ensemble properties of the OA, rather than to its detailed molecular composition, focusing on two quantities in particular, the amount and the oxidation state of the particle-phase carbon. Heterogeneous oxidation increases the oxidation state of particulate carbon, with the rate of increase determined by the detailed chemical mechanism. At the same time, the amount of particle-phase carbon decreases with oxidation, due to fragmentation (C−C scission) reactions that form small, volatile products that escape to the gas phase. In contrast to the oxidation state increase, the rate of carbon loss is nearly uniform among most systems studied. Extrapolation of these results to atmospheric conditions indicates that heterogeneous oxidation can have a substantial effect on the amount and composition of atmospheric OA over timescales of several days, a prediction that is broadly in line with available measurements of OA evolution over such long timescales. In particular, 3−13% of particle-phase carbon is lost to the gas phase after one week of heterogeneous oxidation. Our results indicate that oxidative aging represents an important sink for particulate organic carbon, and more generally that fragmentation reactions play a major role in the lifecycle of atmospheric OA.

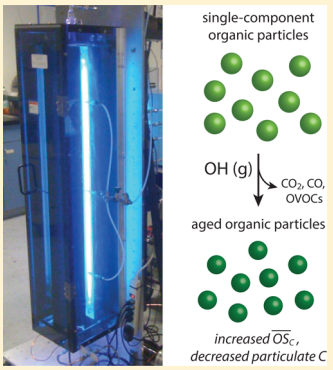

INTRODUCTION

Organic aerosol (OA) makes up ∼50% of fine particulate mass in the Earth's atmosphere[1,2] and thus plays important roles in global climate and human health. Atmospheric OA is an immensely complex organic mixture, made up of thousands (or more) of individual molecules; this complexity arises from the large number of OA sources (both anthropogenic and biogenic), the large number of organic compounds that each source may contribute, and, perhaps most importantly, the reactivity of the constituent organic compounds. All atmospheric organic carbon is subject to oxidation, and since a single oxidation reaction will generally form multiple products, atmospheric oxidation reactions greatly increase the chemical complexity of a given mixture.[3,4] Moreover, oxidation reactions of organic species can dramatically change the reactivity, amount, and properties—and hence the ultimate impacts—of atmospheric aerosol.

The oxidative chemistry controlling atmospheric OA is an important topic lying at the junction of atmospheric and physical chemistry, since the ability to predict and model both the amounts and the climate- and health-relevant properties of the aerosol requires the understanding of the multiphase reactivity (kinetics, mechanism, and products) of organic species. However, our ability to describe this reactivity is currently limited by the very large number of chemical species, reactive transformations, and reaction products involved. This is the case for other highly complex and reactive mixtures of organic species as well, such as organic matter within soils and aquatic systems, soot particles from combustion, and fossil fuel mixtures.

Such immense chemical complexity poses particular challenges for measurements and descriptions of OA on the detailed molecular level. The explicit treatment of a reactive system in terms of all its constituent chemical species generally requires the identification and quantification of each species, the study of each species' reactivity, and the explicit inclusion of all relevant species and reactions within a model. For simple kinetic systems, such an approach is challenging but feasible. However, for highly complex systems such as OA, this approach encounters considerable analytical, experimental,

Received: July 17, 2015
Revised: September 8, 2015
Published: September 18, 2015

DOI: 10.1021/acs.jpca.5b06946
J. Phys. Chem. A 2015, 119, 10767−10783

Table 1. Carbon Atom Bonding for Each Possible Value of OS_C[a]

OS_C	-4	-3	-2	-1	0	+1	+2	+3	+4
n_C=1	CH_4		CH_3OH		CH_2O		CO HCOOH		CO_2
n_C>1				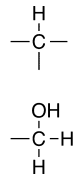	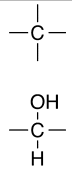	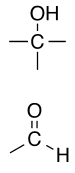			

[a]Structures shown assume only bonds between carbon and C, O, and H; bonds between C and other electronegative atoms (N, S, Cl, etc.) have the same effect as C−O bonds. For example, the carbon atom in a nitrile group has an OS_C of +3.

and computational limitations. While recent advancements in measurement techniques,[5,6] laboratory approaches,[7] and model schemes[3] have greatly improved our ability to understand and describe OA chemistry in terms of individual species, major challenges associated with quantification and carbon closure remain. Moreover, even if the molecular composition and chemistry of OA were fully understood, the computational requirements of most chemical transport models (CTMs) are sufficiently high that detailed, speciated descriptions of OA are not currently feasible. In fact, a molecular-level description of the evolving composition of OA is not always necessary, given that many of the key OA quantities of interest—such as total particle mass and water-uptake properties—derive not from the individual molecules but from their overall average or sum.

An alternative approach for describing the chemistry of complex mixtures such as OA is its treatment not in terms of the detailed structures and reactivity of individual molecules, but rather in terms of the key properties of the organic species or even of the mixture as a whole. The advantage of this "ensemble approach" is that it greatly simplifies the measurement and description of both the chemical composition and reactivity of OA, enabling their relatively straightforward inclusion in CTMs. Such simplified treatments of OA chemistry typically involve the description of organic species or mixtures in terms of two or three average chemical or physical properties (carbon number, elemental ratios, volatility, polarity, carbon oxidation state, etc.), allowing OA or its components to be defined and visualized based on their location in a two- or three-dimensional chemical space.[4,8−14] Understanding how a molecule or mixture changes upon oxidation (corresponding to movement through these spaces) is critical for describing and modeling its atmospheric behavior and thus for predicting the amount, properties, and impacts of OA.

The majority of laboratory studies of OA chemistry focus on the reactions underlying the initial formation and growth of secondary organic aerosol (SOA),[15,16] and results from such studies have recently been used to parametrize simple two-dimensional representations of OA chemistry.[10,11] However, less is known about the chemistry that drives the further evolution ("aging") of OA over its atmospheric lifetime.[17,18] Ambient measurements have shown that even after aerosol growth has essentially stopped (which typically occurs ∼1 d after emission of the organic precursors[19]), OA continues to evolve chemically over timescales of several days,[20−22] indicating that such aging reactions may play an important role in the regional- and global-scale impacts of the aerosol. Since the atmospheric lifetime of OA is 5−10 d,[23] such OA-aging reactions can involve several generations of oxidation. Furthermore, oxidation may occur in different phases, including in the gas phase (homogeneous oxidation of gaseous semivolatile OA components),[24] at the gas-particle interface (heterogeneous oxidation by gas-phase oxidants),[25,26] and within the condensed phase (e.g., homogeneous oxidation within particles, such as deliquesced atmospheric particles or droplets).[27] Regardless of the medium in which oxidation occurs, laboratory measurements of the rates and products of these aging reactions are somewhat limited, in part because of the long timescales and low oxidant concentrations involved; moreover, measurements of multigenerational aging processes have generally not been parametrized for use in simple chemical frameworks or CTMs. Thus, the detailed role of aging reactions in modifying the amounts, composition, and properties of atmospheric OA remains poorly constrained.

In this work we describe (and reanalyze) results from a series of studies performed in our laboratories on the heterogeneous oxidation of organic aerosol by gas-phase OH (the dominant oxidant in the atmosphere). Experiments used various single-component particles, intended as simple model systems for understanding this class of atmospheric aging reaction. Results from all systems are presented on a common basis in terms of both kinetics and products, to provide insight into the overall effect of heterogeneous oxidation on OA, as well as to determine simple parametrizations for inclusion of these reactions in models. In particular we focus on two fundamental properties of OA, the amount and oxidation state of the particulate carbon, key quantities for simple ensemble-based descriptions of OA chemistry. These are discussed in detail in the following section, followed by descriptions of the laboratory experiments, analysis, and results. A simple parametrization of the laboratory results is then presented, allowing for estimates of the effects of heterogeneous oxidation on the amount and oxidation state of particle-phase carbon over its lifetime in the atmosphere. These estimates generally agree with ambient observations. They indicate the importance of heterogeneous oxidation as an atmospheric aging mechanism, and moreover the importance of chemical degradation of OA over multiday timescales.

AMOUNT AND OXIDATION STATE OF PARTICULATE ORGANIC CARBON

In this work we describe OA as an ensemble, representing its composition and reactivity not in terms of its constituent molecules but rather in terms of its organic carbon. Our particular focus is on two ensemble quantities for describing the chemistry of OA, the amount and degree of oxidation of the particle-phase organic carbon, simple parameters that provide

DOI: 10.1021/acs.jpca.5b06946
J. Phys. Chem. A 2015, 119, 10767−10783

basic information about the mass and composition of OA. The extent of oxidation is expressed in terms of the oxidation state of the carbon atom (OS_C),[4] a quantity that (by definition) will increase when the carbon atom undergoes an oxidation reaction. For a single carbon atom bonded to only C, H, and O atoms, OS_C is given by

$$OS_C = n_{C-O} - n_{C-H} \quad (1)$$

where n_{C-O} and n_{C-H} are the number of bonds to O and H, respectively, of the carbon atom in question. (This can easily be generalized to include the effects of heteroatoms such as N, S, Cl, etc.) OS_C values range from −4 to +4, with possible bonding combinations for each value shown in Table 1. How a single oxidation reaction changes n_{C-O} and n_{C-H} thus determines the oxidation state change (ΔOS_C) for that oxidation reaction (Table 2).

Table 2. Changes to OS_C, $\overline{OS}_C$, and Elemental Ratios As a Result of Common Functionalization and Fragmentation Reactions

Reaction type	note	ΔOS_C	$\Delta\overline{OS}_C$	Δ(O/C)	Δ(H/C)
functionalization reactions (saturated molecules)					
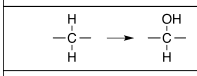		+2	$+2/n_C$	$+1/n_C$	0
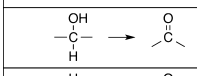		+2	$+2/n_C$	0	$-2/n_C$
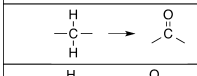		+4	$+4/n_C$	$+1/n_C$	$-2/n_C$
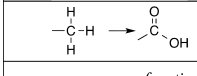		+6	$+6/n_C$	$+2/n_C$	$-2/n_C$
functionalization reactions (unsaturated molecules)					
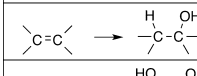	*a, b*	-1, +1	0	$+1/n_C$	$+2/n_C$
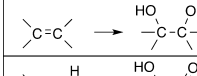	*a*	+1, +1	$+2/n_C$	$+2/n_C$	$+2/n_C$
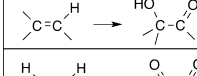	*a*	+1, +3	$+4/n_C$	$+2/n_C$	0
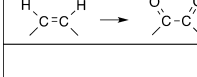	*a*	+3, +3	$+6/n_C$	$+2/n_C$	$-2/n_C$
fragmentation reactions					
	*c*	+1	$+\frac{1}{n_C - \Delta n_C}$	$+\frac{1}{n_C - \Delta n_C}$	$+\frac{1}{n_C - \Delta n_C}$
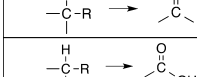	*c*	+3	$+\frac{3}{n_C - \Delta n_C}$	$+\frac{1}{n_C - \Delta n_C}$	$-\frac{1}{n_C - \Delta n_C}$
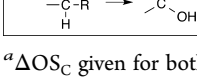	*c*	+5	$+\frac{5}{n_C - \Delta n_C}$	$+\frac{2}{n_C - \Delta n_C}$	$-\frac{1}{n_C - \Delta n_C}$

[a] ΔOS_C given for both carbon atoms in the double bond. [b] Hydration; not an oxidation reaction. [c] $\Delta\overline{OS}_C$, Δ(O/C), and Δ(H/C) are computed only for the fragment without the leaving R group; values given are averages, assuming that both fragments have the same elemental ratio as the parent species (prior to addition of the functional group).

With the exception of techniques that provide detail about the immediate chemical environments of carbon (e.g., NMR,[28] XPS,[29] and STXM[30]), most analytical techniques cannot resolve the OS_C values of individual carbon atoms within organic species. However, techniques that provide measurements of elemental ratios can be used to determine the average carbon oxidation state ($\overline{OS}_C$) of an organic molecule or mixture, since

$$\overline{OS}_C = 2O/C - H/C \quad (2)$$

where O/C and H/C are the molar oxygen-to-carbon and hydrogen-to-carbon ratios.[4] Equation 2 is based on simple valence rules and the assignment of a −2 oxidation state for O and a +1 oxidation state for H; the presence of peroxide groups or heteroatoms may introduce some errors to this calculation, though for atmospheric OA such errors are likely to be small.[4]

Since a single oxidation reaction of an organic molecule will typically change the oxidation state of only a fraction of the organic carbon, the change to $\overline{OS}_C$ upon oxidation ($\Delta\overline{OS}_C$) will depend not only on the changes to the C−O and C−H bonding eq 1 but also on the number of carbon atoms in the molecule (n_C). Such changes are given in Table 2, with all oxidation reactions classified as either functionalization or fragmentation reactions. A third class of reaction, oligomerization (not shown in Table 2), is generally a nonoxidative process that occurs after fragmentation or functionalization, and typically involves no changes to $\overline{OS}_C$.

Functionalization reactions involve the addition of functional groups to the carbon skeleton, via the replacement of C−H bonds (or unsaturated/cyclic C−C bonds) with C−O bonds, with no change to n_C. As shown in Table 2, the change to $\overline{OS}_C$ from functionalization is governed by simple rules: replacement of a C−H bond with a C−O bond (as in the case of the addition of an alcohol, peroxide, or nitrate group) increases $\overline{OS}_C$ by $+2/n_C$, whereas replacement of a C−C bond with a C−O bond increases $\overline{OS}_C$ by $+1/n_C$. All effects are additive, so the replacement of a CH_2 group with a C═O group increases $\overline{OS}_C$ by $+4/n_C$, and the oxidation of an alkane to a carboxylic acid or hydroxycarbonyl increases it by $+6/n_C$.

Fragmentation reactions involve a decrease in carbon number n_C, typically through C−C bond scission in an acyclic carbon skeleton. (The scission of one C−C bond within a ring does not change the n_C of the molecule and thus can be considered a functionalization reaction.) Major mechanisms leading to fragmentation are alkoxy radical decomposition,[31] alkene ozonolysis,[32] and carbonyl photolysis;[33] other chemically activated radicals or molecules may also fragment as well.[34,35] The effect of fragmentation on $\overline{OS}_C$ is more complex than that of functionalization, since two products are formed; the value of $\Delta\overline{OS}_C$ (from the perspective of a single fragment) depends on not just the functional group that replaces the C−C bond but also the size and degree of oxidation of the other fragment. The values of $\Delta\overline{OS}_C$, Δ(O/C), and Δ(H/C) listed in Table 2 for fragmentation are averages, calculated using the assumption that (prior to oxygen addition) both fragments retain the elemental composition of the parent species. Because of the decrease in n_C, fragmentation reactions can efficiently increase the $\overline{OS}_C$ of organic species. However, since the fragments will be smaller than the parent compound, such reactions generally lead to an increase in volatility of the organic species.

The detailed dependence of volatility on ensemble chemical composition (described by O/C, H/C, and n_C) is discussed elsewhere.[13] This dependence is important in that volatility is a key determinant of gas-particle partitioning and hence of OA loading. In general, most functionalization reactions lead to a decrease in volatility, due to an increase in polarity, whereas most fragmentation reactions (as well as functionalization reactions that convert one functional group to a less-polar one) will lead to a volatility increase. Such reactions can lead to a loss

DOI: 10.1021/acs.jpca.5b06946
J. Phys. Chem. A 2015, 119, 10767−10783

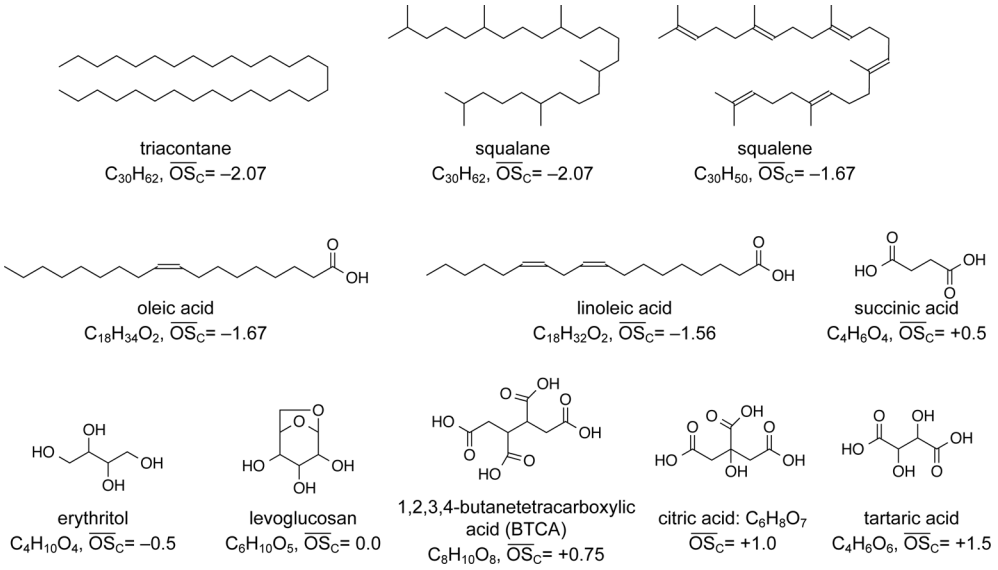

Figure 1. Model single-component OA systems examined in this work.

of organic carbon from the particle phase, which as we show in this work is an important process in the atmospheric aging of OA.

HETEROGENEOUS OXIDATION EXPERIMENTS

Over the last several years our groups have studied the heterogeneous oxidation of organic particles by OH as model systems for understanding how OA undergoes oxidative aging in the atmosphere. These studies complement work by a number of other laboratories, aimed at understanding the kinetics and products of heterogeneous reactions of gas-phase radicals with condensed-phase organic compounds. Heterogeneous oxidation chemistry was recently reviewed by George and Abbatt;[25] briefly, laboratory studies have focused on the kinetics of oxidation (specifically, measurements of the uptake coefficient γ, the fraction of radical–particle collisions that lead to reaction),[36−50] the oxidation products in the particle phase,[39,42,45,51−58] the evolving properties of the aging OA,[59−63] and the loss of OA mass via the formation of small, volatile products.[38,41,42,51,52,64−66] This last topic—the role of heterogeneous oxidation as an OA sink—is still poorly understood, as the observed extent of chemical degradation varies widely from study to study. More generally, despite the substantial chemical insight that these studies provide, the overall role that heterogeneous oxidation plays on atmospheric OA remains poorly constrained, since its effects on OA composition and chemistry have not been described or parametrized generally. As a result, heterogeneous oxidation reactions have been included in only a handful of CTM treatments to date.[67,68]

The studies described here focus on the OH oxidation of single-component organic particles. We have also examined the heterogeneous oxidation chemistry of complex aerosol mixtures (SOA,[17] diesel exhaust,[69] fulvic acid,[70] and soot[71]), as have other researchers,[54,55] but single-component systems offer several advantages in terms of data analysis and interpretation. They ensure that the chemical properties of the starting material are well-defined, plus they provide a relatively straightforward means for quantifying the heterogeneous oxidation kinetics (as described below). Furthermore, since the unreacted OA starts out chemically simple, but increases in chemical complexity as oxidation proceeds, these reactive systems represent intermediate steps toward the immense chemical complexity encountered in SOA and ambient OA. Finally, heterogeneous oxidation is an ideal system for studying the oxidation chemistry of organic species generally, since modern online aerosol chemistry instruments can quantitatively measure all organic carbon in the particle phase, allowing for the overall, comprehensive study of its evolution upon oxidation. This includes highly oxidized species, which have traditionally been challenging to measure and study in the gas phase.

EXPERIMENTAL SECTION

All measurements described here are from our previously published studies of the heterogeneous oxidation of single-component particles.[4,56,70,72−76] The 11 precursors studied, shown in Figure 1, span a wide range of chemical species, including reduced, saturated compounds (squalane[72,73] and triacontane[4]), compounds containing C=C double bonds (oleic acid, linoleic acid, and squalene[56,75]), polyols (erythritol and levoglucosan[74]), and multifunctional organic acids (succinic acid,[76] 1,2,3,4-butanetetracarboxylic acid (BTCA), citric acid, and tartaric acid[70]). Only one previously reported compound, linolenic acid,[75] is not included in this analysis, due to the apparent importance of SOA formation in that case, an interference that precludes the analysis used here.

Detailed experimental procedures, which are quite similar for all compounds studied, can be found in the appropriate references; only a brief overview, and details of the analysis unique to the present work, are given here. A schematic of the experimental setup is shown in Figure 2. Single-component organic particles (polydisperse distributions, with surface-weighted average diameters ranging from ∼125 to ∼300 nm) were generated from atomization/nebulization of an aqueous solution followed by drying, or from homogeneous nucleation from heating the pure organic compound in a tube furnace. Particles then entered a flow tube where they were subject to oxidation by gas-phase OH. Two different quartz flow reactors were used; one (for squalane, triacontane, erythritol, levoglucosan, tartaric acid, BTCA, citric acid, and succinic acid) of 130 cm length and 2.5 cm ID (residence time 37 s) and

DOI: 10.1021/acs.jpca.5b06946
J. Phys. Chem. A 2015, 119, 10767−10783

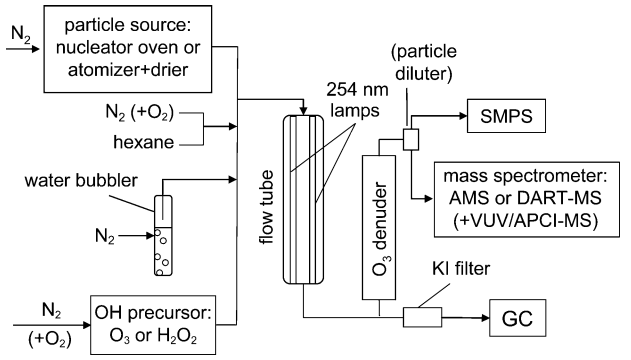

Figure 2. Schematic of the experimental setup for all heterogeneous oxidation experiments. Parentheses indicate components/flows that were not used in all experiments.

the other (for squalene, oleic acid, and linoleic acid) of 170 cm length and 6.5 cm ID (residence time 224 s). Carrier flow was 5−10% O_2 in N_2, at ∼30% relative humidity (RH; 64% RH for succinic acid). For most compounds, OH was produced from ozone photolysis. O_3 was generated prior to the flow reactor using a mercury pen-ray lamp or corona discharge, and photolyzed by 254 nm light from mercury lamps external to the flow; the subsequent $O(^1D)+H_2O$ reaction then generated OH to initiate oxidation. For the alkene experiments (oleic acid, linoleic acid, and squalene), to avoid ozonolysis chemistry, OH was instead generated from the photolysis of H_2O_2, which was added to the reactor by passing nitrogen through urea hydrogen peroxide. The OH concentration in the flow tube was varied by changing the concentration of added O_3 or H_2O_2 or by changing the UV photon flux into the flow tube. OH exposures were monitored by measuring the decay of a gas-phase OH tracer (hexane) using a gas chromatograph with flame ionization detection (GC-FID);[72] OH concentrations in the reactor varied from 8×10^7 to 8×10^{11} molecules per cubic centimeter. At these high concentrations, oxidation by OH is generally much more rapid than 254 nm photolysis.[77]

The changes in chemical composition of the particles were measured by high-resolution mass spectrometry. Oxidation state of the OA was determined from eq 2, using online measurements of elemental ratios (O/C and H/C). For all systems studied except succinic acid, measurements were made using an Aerodyne high-resolution time-of-flight mass spectrometer (AMS),[78] which utilizes electron impact (EI) ionization, a hard-ionization technique for describing the ensemble chemical composition of OA. AMS measurements of elemental ratios require empirical correction factors to account for biases in ion fragmentation;[79−81] our previous studies utilized the original correction factors of Aiken et al.,[80] though revised factors, based on a larger set of organic standards, were recently put forth by Canagaratna et al.[81] For most data sets we updated our elemental ratio values with these new factors. However, for the polyfunctional species, updated O/C measurements remained somewhat lower than the actual values, a result consistent with the data of Canagaratna et al.[81] In addition, measured H/C values for the alkanes (squalane and triacontane) were somewhat overestimated. Thus, for each individual data set, O/C and H/C were adjusted by empirical multiplicative factors to give the correct value for the pure compound, and these factors were applied across the entire heterogeneous oxidation experiment. We note, however, that the overall results of this study are largely unaffected by this choice of correction factor.

Because heterogeneous oxidation can lead to the loss of particle-phase organic carbon via volatilization reactions, an important parameter in these experiments is the fraction of particulate carbon f_C remaining after oxidation. For the AMS experiments, this was calculated from changes to the mass of the particulate organic carbon, which in turn was determined from the mass and elemental ratios of the OA:

$$f_C = \frac{m_C(\text{reacted})}{m_C(\text{unreacted})} \qquad m_C = m_{OA}\left(\frac{12}{12 + 16O/C + H/C}\right) \tag{3}$$

where m_C and m_{OA} are the particle-phase carbon mass and organic mass, respectively (normalized by particle number concentration, to account for potential changes in the particle source). Total ion signal from the AMS was found to be an unreliable measure of m_{OA}, exhibiting dependences on particle shape and degree of oxidation; in particular, ion signal generally decreased dramatically at high OH exposures, suggesting decreases in AMS collection efficiency. Thus, m_{OA} was instead determined from scanning mobility particle sizer (SMPS) measurements of particle volume multiplied by the effective density (ratio of the vacuum aerodynamic diameter and aerodynamic diameter, measured by the AMS and SMPS, respectively).[82]

For succinic acid,[76] particle chemistry was instead measured using a soft ionization technique, direct analysis in real-time (DART) with ultrahigh resolution mass spectrometry. Unlike the AMS, DART produces molecular ions, providing the exact formulas of individual chemical components of the aerosol. Here such molecular results are converted to average elemental ratios and fraction of carbon remaining by assuming that the ion signals reflect populations of individual molecules in the aerosol.[76]

Heterogeneous oxidation kinetics, discussed in detail in the Results Section, are constrained using measurements of the reactive loss of the precursor molecule. Different mass spectrometric techniques were used for different chemical systems. Soft ionization schemes, enabling measurements based on the intensity of the (quasi-)molecular peak, include DART (for succinic acid), atmospheric pressure chemical ionization (APCI, for oleic acid and linoleic acid), and vacuum ultraviolet ionization (VUV, for squalene). The APCI and VUV measurements were performed in separate experiments as the EI-AMS product studies, necessitating interpolation of the kinetic decays in those cases. The remaining species were measured by hard ionization (EI-AMS), so an EI tracer ion was used instead. The EI tracer ion for each precursor was selected based on its fast rate of decay upon heterogeneous oxidation, and a high signal-to-noise ratio, relative to other ions in the mass spectrum. For oleic acid, linoleic acid, and squalene, the EI tracer-ion technique gives slower decays than the soft ionization measurements, possibly due to product mass spectra that also contain the tracer ion. However, this technique has been used to measure reasonably large uptake coefficients ($\gamma > 0.5$),[74] and moreover EI and VUV measurements of squalane decays agree extremely well with each other.[72] Thus, while the use of EI tracer ions seems to underestimate the loss rate of the alkenes, this does not appear to be a general effect for other systems.

DOI: 10.1021/acs.jpca.5b06946
J. Phys. Chem. A 2015, 119, 10767−10783

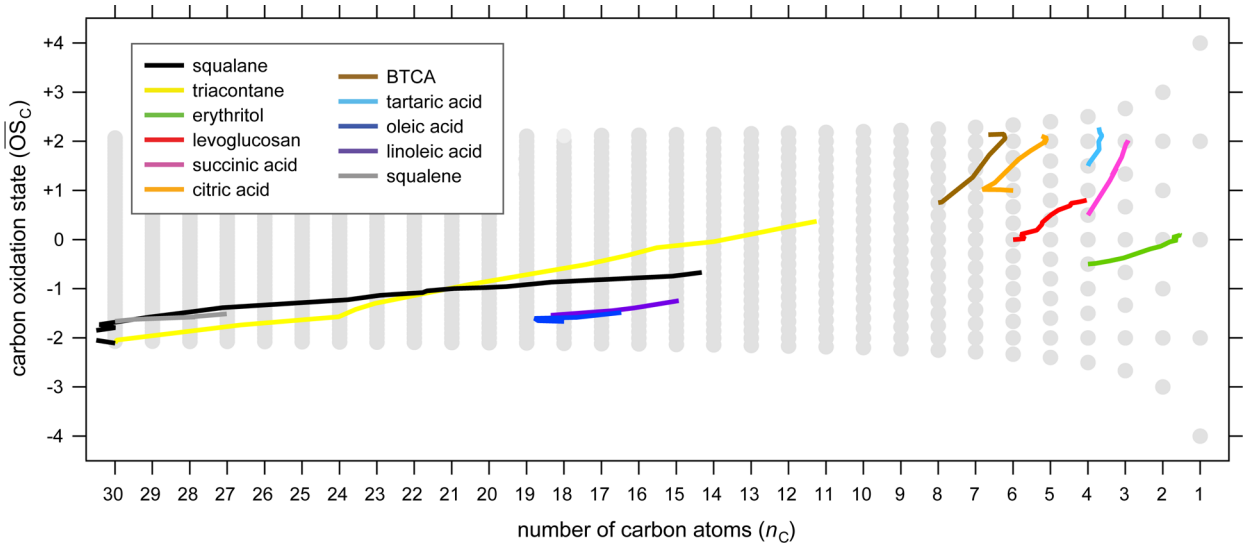

Figure 3. Changes to $\overline{OS}_C$ and n_C for all heterogeneous oxidation experiments. Movement in this two-dimensional chemical space is upward and to the right, as expected for oxidation reactions.[4] Gray circles indicate possible combinations of $\overline{OS}_C$ and n_C. For all experiments except succinic acid (for which n_C is measured directly), the decrease in n_C is assumed to be proportional to the loss of carbon from the particle.

RESULTS AND DISCUSSION

Chemical Changes to the Organic Aerosol. The ensemble chemical changes that the different single-component aerosol types undergo upon heterogeneous oxidation are shown in Figures 3 and 4. Data are presented in terms of changes to four key ensemble quantities ($\overline{OS}_C$, n_C, O/C, and H/C), with changes shown as movement in two chemical spaces, both of which we have used previously to describe product formation in our experiments.

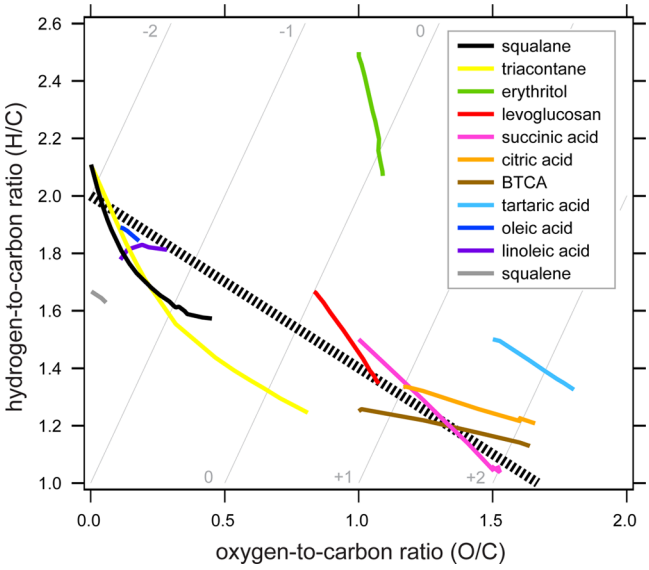

Figure 4. Changes to O/C and H/C for all heterogeneous oxidation experiments. In most cases O/C increases and H/C decreases, moving the OA toward the bottom right of the plot; however, the actual paths taken (the slopes in this chemical space) are highly precursor-dependent. For comparison, ambient OA tends to fall along a slope of ca. −0.6 (dashed line).[84] Gray lines denote contours of constant $\overline{OS}_C$.

Figure 3 shows particle evolution in $\overline{OS}_C$-n_C space for the various systems studied. This chemical space is discussed in detail elsewhere;[4] briefly, oxidation drives organic species upward and to the right, toward CO_2 (OS_C = +4), via both functionalization reactions (upward movement only) and fragmentation reactions (upward and rightward movement). In the present study $\overline{OS}_C$ is always measured directly, but for most experiments n_C is not, since carbon number cannot be measured using EI-AMS (a hard ionization technique). For those experiments n_C is estimated by assuming that the loss of carbon from the particle is governed by a decrease in the average carbon number of the constituent molecules.[4] This is strictly true only if the number of molecules within the particle remains constant, with all fragmentation reactions leading to the loss of one small, volatile fragment (CO_2, CO, and small oxygenated volatile organic compounds, OVOCs), with the other less-volatile one remaining in the particle. This may not always be the case, since there is a possibility that both fragmentation products (or neither fragmentation product) may be lost to the gas phase, which would imply changes in n_C that are not directly related to changes in the amount of particulate carbon. Indeed, as described below, the formation of two volatile fragments appears to drive the observed changes to erythritol particles. However, volatility measurements suggest that carbon loss from squalane particles arises from the loss of small, volatile fragmentation products,[73] suggesting that our assumption relating n_C and f_C is valid in at least some cases.

The trajectories shown in Figure 3 cover a large fraction of $\overline{OS}_C$-n_C space, occupying a diagonal swath that ranges from large, chemically reduced compounds (lower left corner) to small, oxidized ones (upper right corner). This overlaps well with the area of chemical space occupied by atmospheric OA, which falls along this same diagonal.[4,13] Small, reduced compounds are too volatile to be present in the condensed phase, whereas large, highly oxidized species (n_C > 10, $\overline{OS}_C$ > +0.5) are generally not observed. Taken together, the oxidation trajectories tend to curve upward, with the largest $\overline{OS}_C$ increases for the smallest molecules. This is because n_C controls the extent to which the oxidation of a single carbon atom will affect the average $\overline{OS}_C$ of the whole molecule (Table 2). The decrease in inferred n_C in all cases indicates the

DOI: 10.1021/acs.jpca.5b06946
J. Phys. Chem. A 2015, 119, 10767−10783

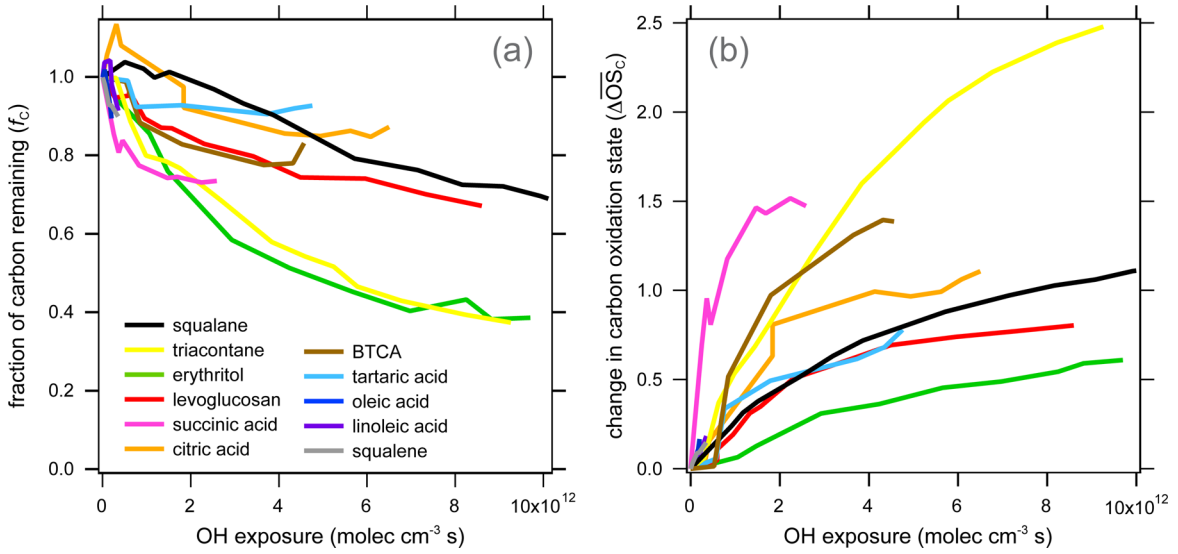

Figure 5. Fraction of carbon remaining in the particle phase (a) and changes in particulate $\overline{OS}_C$ (b) as a function of OH exposure. Both exhibit considerable variability among different species, since heterogeneous oxidation kinetics depend on a number of physical and chemical properties of the particles (eq 4). The curvature observed for most systems indicates that oxidation slows at higher OH exposures, likely due to changes in reactivity or viscosity of the OA components.

importance of carbon loss by fragmentation reactions, which is discussed in more detail below.

Figure 4 shows the trajectories that the particles take in Van Krevelen (H/C vs O/C) space, a chemical space that has seen substantial use for describing ensemble chemical changes to OA.[9,83,84] This provides more information on OA composition than $\overline{OS}_C$-n_C space, since the functional group distributions and changes can be estimated from relative oxygen, hydrogen, and carbon contents[9,13] (see Table 2); however, such detail comes at the expense of information on carbon number, and fragmentation and functionalization reactions cannot be easily distinguished in this two-dimensional space. For comparison, Figure 4 also shows the average of Van Krevelen slopes from a large number of ambient OA measurements.[84]

Most starting materials used in this study, and their oxidation trajectories, fall reasonably close to the ambient range (as is the case in Figure 3). The main exception is erythritol, which has a higher H/C than is typically seen for OA; however, it is also chemically similar to C_5 tetrols, major components of isoprene-derived SOA.[85] Additionally, tartaric acid is significantly more oxidized ($\overline{OS}_C$ = +1.5) than most ambient aerosol. Trajectories in most cases do not follow the "ambient slope" (−0.6) exactly, but do show movement toward the bottom right (from a combination of O addition and H loss). Erythritol is again a major exception, as oxidation is governed by H loss, suggesting the importance of oxidation of alcohol groups to carbonyl groups. In addition, linoleic acid shows an initial increase in H/C with oxidation, possibly due to the addition of OH groups to the multiple C═C double bonds in the molecule. Most trajectories are roughly linear in this space, though squalane and triacontane (the two alkanes studied) exhibit some rightwards curvature, suggesting a shift from the addition of carbonyl groups to the addition of alcohol groups.[9] The product trajectories from these two systems fall somewhat below the "ambient line", which was recently shown to be a general feature of laboratory OA studies;[84] however, this is not the case for most other systems studied here, suggesting that this effect may be precursor-dependent.

Rates of Organic Aerosol Transformation. While the trajectories in Figures 3 and 4 provide information about the products of the heterogeneous oxidation of particulate organic species, they provide no information as to the rates of the reactions, which is necessary for modeling the chemistry and impacts of OA aging. In this section we examine such rates, with a focus not on the reactive loss kinetics of the parent species but rather on the rate at which the particulate organic carbon changes with oxidation.

The changes to the average carbon oxidation state ($\Delta\overline{OS}_C$) and fraction of carbon remaining in the particle phase (f_C), obtained from eqs 2 and 3, respectively, are shown in Figure 5 as a function of OH exposure. For all systems studied, oxidation leads to an increase in $\overline{OS}_C$ of the particulate carbon, as expected, as well as a decrease in f_C. While changes are for the most part monotonic, some minor deviations are observed, likely due to noise in the ion signal and/or variations in the particle source. For example, the initial spike in f_C for citric acid is due to fluctuations in the atomizer output. Such fluctuations contribute to the errors in the parametrization of results, which is discussed in a later section. Regardless, the loss of particulate carbon with oxidation (Figure 5a) is seen for all systems studied, indicating the formation of volatile products via C−C scission reactions. Such fragmentation reactions presumably involve alkoxy (RO) radicals (formed from RO_2+RO_2 reactions), most importantly "activated" alkoxy radicals in which the radical center is adjacent to a functional group, promoting C−C bond scission.[31,86] Less-volatile fragments will remain in the condensed phase, contributing to the increase in particle $\overline{OS}_C$ (Figure 5b); however, the observation of products of the same carbon number as the parent species[72,76,87] indicates the importance of functionalization reactions as well, at least for the early generations of oxidation.

Heterogeneous oxidation thus leads to the formation of oxidized species in both the particle and gas phases. However, these results alone provide limited direct insight into the rates at which these products will be formed in the atmosphere. The kinetics are determined not only by reactivity—described by

DOI: 10.1021/acs.jpca.5b06946
J. Phys. Chem. A 2015, 119, 10767−10783

the uptake coefficient γ, the fraction of OH-surface collisions that result in reaction—but also by physical parameters that determine the availability of aerosol components at the particle surface, such as particle size, density, and viscosity.[44,72] Such dependences contribute to the large variability in the rate of OA evolution seen in Figure 5. In the past we have accounted for these dependences by describing kinetics in terms of the number of "oxidation lifetimes" of the parent species,[72] the average number of reactions with OH that each molecule in the particle has undergone. Assuming rapid mixing within the particle, the lifetime of a particle-phase molecule versus heterogeneous oxidation by OH (τ_{molec}) is given by

$$\tau_{molec} = \frac{\text{number of molecules in particle}}{\text{rate of reaction at the particle surface}} = \frac{VN_a\rho/M}{1/4\gamma\bar{v}[OH]S} = \frac{2N_a\rho}{3\gamma\bar{v}[OH]M}D_p \quad (4)$$

where V is the particle volume, N_a is Avogadro's number, ρ is the density of the particle, M is the molecular weight, γ is the uptake coefficient, $\bar{v}$ is the mean molecular speed of the oxidant (609 m/s for OH at 298 K), [OH] is the gas-phase concentration of the hydroxyl radical, S is the particle surface area, and D_p is the particle diameter. The rate of heterogeneous oxidation thus depends critically on the surface area-to-volume ratio: because molecules within the particle bulk are largely "shielded" from gas-phase oxidants, heterogeneous oxidation rates are generally slower than gas-phase rates, especially when the particles are large. (The final equality in eq 4 assumes the particles are spherical.) The number of molecular lifetimes, or the average number of reactions a particle-phase molecule has undergone by time t, is therefore

$$\text{lifetimes}_{molec} = \frac{t}{\tau_{molec}} = \frac{3\gamma\bar{v}M}{2N_a\rho D_p}[OH]t \quad (5)$$

in which $[OH]t$ is the OH exposure. In a given experiment, all terms in eq 5 are known except for the uptake coefficient γ. This is typically determined from the initial rate of decay of the parent organic compound, as measured by aerosol mass spectrometry. However, as shown in Figure 6, in many cases the rate of decay of the parent species deviates from the expected exponential behavior (solid lines) and instead decreases at higher OH exposures. This kinetic "slowing" of oxidation, which has been observed by other researchers as well,[41,S1] may arise not only from changes to the parameters in eq 5 but also from diffusive limitations in the particle, limiting the ability of molecules located inside the particle to react at the surface on the timescale of the OH collision. Such diffusive limitations depend upon particle viscosity, particle size, and collision rate of OH with the surface.[44,88]

Because of this kinetic slowing, the use of eq 5, with fixed parameters from the initial decay, will lead to overestimates of the average rate of oxidation of the particulate organic species over the full OH exposure accessed in the experiments. To account for this slowing, we thus estimate lifetimes directly from the decrease in parent concentration (ion signal). Signals versus OH exposure are fit to a biexponential decay (dashed curves in Figure 6), and the number of lifetimes at a given exposure is determined from $-\ln[S]/[S]_0$, in which $[S]/[S]_0$ is the ratio of the fitted ion signal at that exposure to the original ion signal in the unreacted particles. This provides a direct measure of the rate of oxidation of the parent organic compound; if product species react similarly (which has been observed for some compounds[72,89]), this approach also accounts for changes in their kinetics as well. This assumes some degree of mixing within the particle on the timescales probed, and cannot specifically account for reactions on solid particles for which no surface replenishment of reactants occurs. It is also limited to measurements of only the first ~3−4 molecular lifetimes, since beyond that the parent species cannot be quantified accurately.

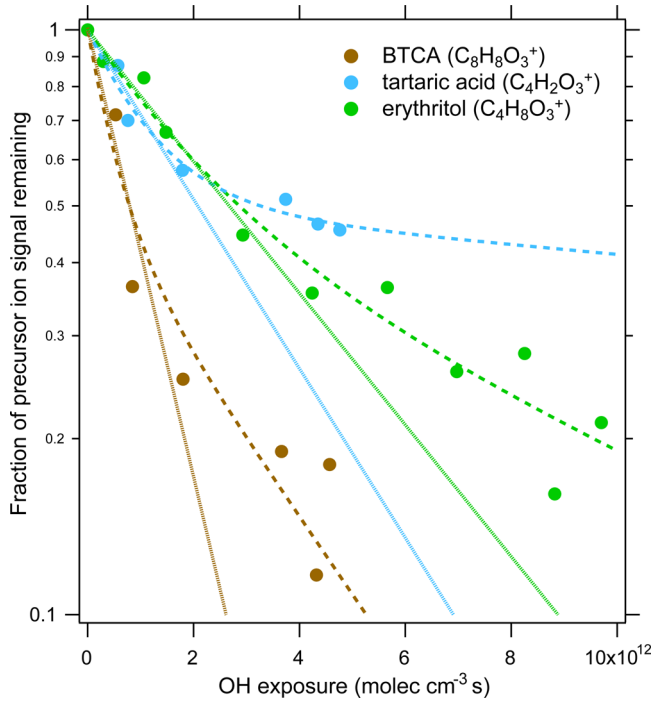

Figure 6. Decays of ion signal for three single-component aerosol types as a function of OH exposure. Circles are normalized intensities of high-resolution EI tracer ions, corrected for changes in particle mass. Solid curves are exponential fits to the initial decay (first 4−6 data points) of a given species; dashed curves are biexponential fits to all measurements of a given species, so that any slowing of the reaction can be explicitly taken into account. Y-intercepts are set to 1 for all fits.

Results ($\Delta\overline{OS}_C$ and f_C vs molecular lifetimes) are given in Figure 7. The measurements exhibit substantially less curvature than in Figure 5, due to the kinetic correction described above. The slopes in both plots, which reflect average changes to $\overline{OS}_C$ and f_C per reaction, exhibit substantial variability among the different chemical systems studied. Much of this variability can be attributed to differences in carbon chain length (n_C), with the smallest molecules generally exhibiting the largest slopes, since the effect of a given oxidation reaction is inversely proportional to n_C (Table 2). However, there are some exceptions to this overall trend, which are likely related to details of the chemical mechanism and/or partitioning of the reaction products. For example, the unsaturated species (oleic acid, linoleic acid, and squalene) exhibit $\overline{OS}_C$ increases that are consistent with each other but that are slower than the saturated species; this is likely due to the importance of secondary reactions that lead to less-functionalized products.[56,75,87] In addition, erythritol particles, which lose carbon rapidly due to the small size of the erythritol molecule, exhibit a relatively slow increase in $\overline{OS}_C$. This effect likely results from the high volatility of the reaction products, which include C_4 species formed from the alcohol-to-carbonyl functionalization

DOI: 10.1021/acs.jpca.5b06946
J. Phys. Chem. A 2015, 119, 10767−10783

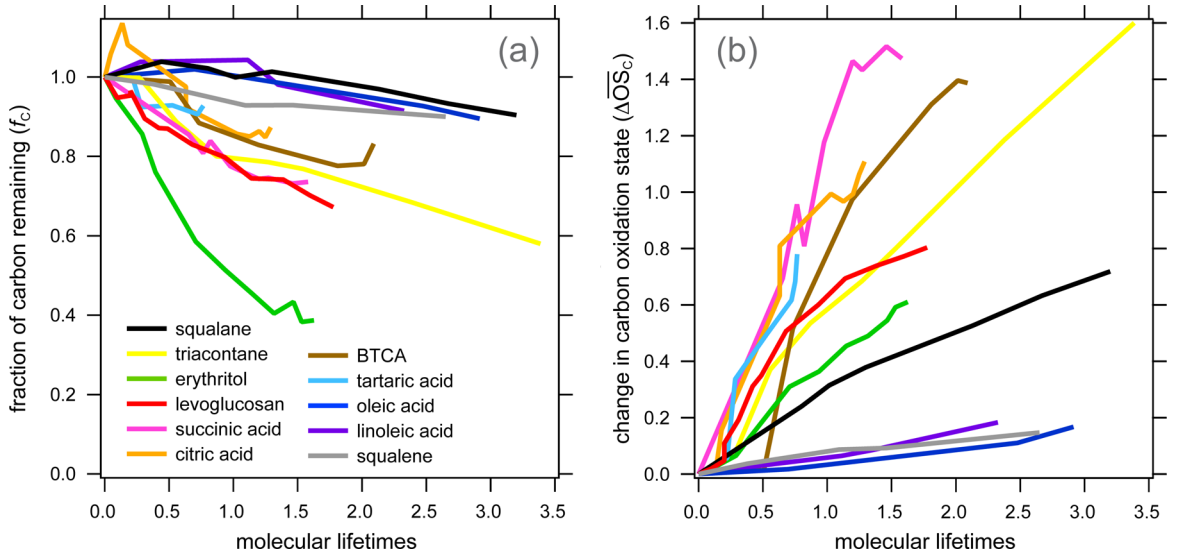

Figure 7. Fraction of carbon remaining in the particle phase (a) and changes in particulate $\overline{OS}_C$ (b) as a function of molecular lifetimes. Much of the observed variability among systems arises from differences in molecular size (n_C), with the smallest molecules undergoing the largest changes per reaction; however, there are exceptions (see text).

reactions (Figure 4), and more importantly C_1−C_3 fragmentation products. This increase in volatility will cause the loss of all the carbon in the molecule to escape to the gas phase, leaving relatively few oxidation products in the particle phase. (This is consistent with the close correspondence between erythritol loss and particle mass loss during oxidation.[74]) The other C_4 species (tartaric and succinic acids) are likely to form products that are lower in volatility than those from erythritol, so carbon loss is not as dramatic, and the increase in $\overline{OS}_C$ is more rapid. Finally, triacontane (a C_{30} *n*-alkane) exhibits behavior that is fundamentally different than any of the other species, undergoing changes to f_C and $\overline{OS}_C$ that are as rapid as much smaller (C_{4-6}) compounds. The reason for this rapid oxidation is unclear, but it may be a result of the solid crystalline phase of the particles and the strong surface alignment of molecules.[57] By contrast, the other species studied are either liquids at room temperature or are very hygroscopic and likely exist in semisolid or aqueous states at the RH levels of these experiments.[90]

Differences in the oxidation mechanism and partitioning therefore account for some fraction of the variability seen in Figure 7. Nonetheless, most of the variability results from differences in the size of the carbon skeleton (n_C) of the parent organic species. To account for this dependence, here we introduce a new metric for heterogeneous oxidation kinetics, "carbon lifetimes", the average number of oxidation reactions that a particulate organic carbon atom has undergone:

$$\text{lifetimes}_{\text{carbon}} = \frac{t}{\tau_{\text{carbon}}} = \frac{t}{\tau_{\text{molec}} n_C} = \frac{\text{lifetimes}_{\text{molec}}}{n_C} \quad (6)$$

This carbon-lifetime metric, which is simply the number of molecular lifetimes divided by n_C, allows the oxidation chemistry to be described in terms of the OA's constituent carbon atoms rather than its constituent organic molecules. As shown in the Implications Section (below), such an ensemble description of the kinetics allows for the straightforward estimation of the effects of heterogeneous oxidation of atmospheric OA, which is far more chemically complex than the single-component systems studied here.

Figure 8 shows f_C and $\Delta\overline{OS}_C$ as a function of carbon lifetimes. The fraction of carbon remaining (Figure 8a) is in close general agreement for most compounds studied. With the exceptions of erythritol and triacontane, which as noted above exhibit unusually rapid carbon loss, all particle types lose particle mass quite uniformly, with a decay constant of 0.84 ± 0.31 per carbon lifetime. (All errors given are 95% confidence intervals, shown as shaded areas; this fit also excludes the alkene species, but their inclusion does not appreciably change the results.) Thus, if a particle (or molecule) is subject to enough oxidation such that each constituent carbon atom experiences on average one OH oxidation reaction, ∼60% of the organic carbon will be lost to the gas phase; equivalently, for each oxidation reaction of a carbon atom, 0.6 carbon atoms are lost from the particle. This does not necessarily imply that a given carbon atom will volatilize 60% of the time it reacts with OH, but rather represents the average behavior of the overall system. Reactions can form volatile fragments spanning a range of carbon numbers (C_1, C_2, C_3, ...), or form no volatile fragments at all; in addition, multiple generations of products can coexist at any given time, which will also affect the average volatilization rate.[89]

The general agreement in the rate of carbon loss for such a wide range of chemical systems suggests that the mechanisms underlying fragmentation/volatilization are similar for most of the organic classes examined here. Within the noise of the individual measurements, the only compounds that show clear deviations from this simple exponential (or initially linear) decay are squalane and oleic acid, which initially exhibits little change in f_C for the first ∼0.05 carbon lifetimes, before carbon loss begins. We interpret this in terms of a shift from functionalization reactions to fragmentation reactions as the molecule becomes increasingly oxidized,[73] which is consistent with the known chemistry of alkoxy radicals.[31] However, the other reduced species studied (squalene, linoleic acid, and triacontane) do not exhibit this same behavior. This may be due to differences in chemical mechanisms, phase/viscosity of the particles, or differing amounts of initial SOA formation. Nonetheless, the changes to f_C in all systems indicate the

DOI: 10.1021/acs.jpca.5b06946
J. Phys. Chem. A 2015, 119, 10767−10783

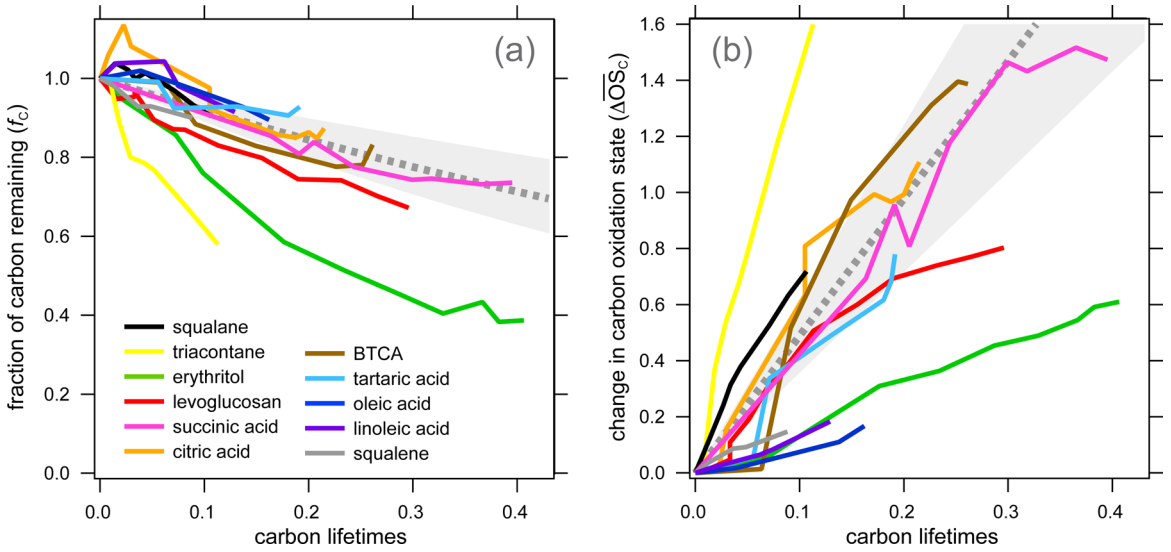

Figure 8. Fraction of carbon remaining in the particle phase (a) and changes in particulate $\overline{OS}_C$ (b) as a function of carbon lifetimes. Carbon loss (from fragmentation reactions) is relatively uniform among most systems studied, whereas oxidation state increase depends more strongly on details of the chemical mechanism. Dashed lines are averages of fits to the exponential decays (a) or linear slopes (b) for six particle types (squalane, levoglucosan, succinic acid, citric acid, BTCA, and tartatic acid), with shaded areas denoting the 95% confidence intervals.

importance of particulate carbon loss via fragmentation reactions during atmospheric aging, as well as the relative uniformity of the rate of this loss on a per-carbon basis.

The increase in particulate $\overline{OS}_C$ with oxidation (Figure 8b) is more variable among different chemical systems than is carbon loss. Each slope represents the average change in oxidation state from the oxidation of a single carbon atom in the particle (i.e., the ΔOS_C values in Table 2); as with carbon loss (Figure 8a), this average value likely involves a range of reactions, carbon atoms in a given molecule, and generation numbers. For all compounds besides triacontane—which, as discussed above, seems to undergo oxidation extremely rapidly—the slopes vary from ca. +1 to ca. +6, spanning the full range of reasonable OS_C changes per reaction (Table 2). The particles that undergo the least amount of oxidation per carbon atom are the unsaturated species (oleic acid, linoleic acid, and squalene) and erythritol. As described above, the slow rate of oxidation of these species can be explained by their known chemistry and volatility. The remaining six species have only C−C single bonds and thus are more chemically similar to ambient OA; these exhibit average slopes of 4.9 ± 1.3 (dashed line), corresponding to the formation of ∼2−3 new C−O bonds per oxidation reaction (see Table 2).

Figure 8 shows that the changes to the amount and the oxidation state of particulate carbon behave fundamentally differently: the rate of carbon loss is essentially uniform across most systems studied, whereas the rate of $\overline{OS}_C$ increase is quite variable. This variability in $\Delta\overline{OS}_C$ results from the differences in the identity and number of functional groups added per oxidation reaction (Table 2), which in turn depends on molecular structure and the detailed reaction mechanism. However, such differences do not appear to have a dramatic effect on the rate of carbon loss (Figure 8a). This is broadly consistent with alkoxy radical reactivity: fragmentation is strongly enhanced when the radical is "activated" (i.e., when an oxygen-containing functional group is located adjacent to the radical center), though the exact identity of the functional group (e.g., carbonyl vs alcohol) plays little role.[31] Thus, the rate of carbon loss from the particle phase is relatively insensitive to the exact functional group distribution within an organic mixture. This may explain the differences in variability seen in Figure 8a,b across all the systems studied; it also provides additional evidence that carbon loss from heterogeneous oxidation is driven by the fragmentation of alkoxy radicals.

IMPLICATIONS

In the experiments described in this work, model OA particles are often subject to much higher OH exposures than atmospheric OA particles are likely to experience over their atmospheric lifetimes (5−10 d on average). Nonetheless, the present results suggest that over this time, atmospheric OA will undergo significant, measurable changes as a result of heterogeneous oxidation. Shown in Figure 9 are estimated changes to the amount and the oxidation state of particle-phase organic carbon within OA as a function of atmospheric residence time. The values shown are from the experimentally determined dependences of $\Delta\overline{OS}_C$ and f_C on carbon lifetimes (fits in Figure 8), and estimated carbon lifetimes, calculated from a modified version of eq 6:

$$\text{lifetimes}_{\text{carbon}} = \frac{\text{lifetimes}_{\text{molec}}}{n_c} = \frac{3\gamma\bar{v}M}{2N_a\rho D_p n_C}[\text{OH}]t$$
$$= \frac{3\gamma\bar{v}(12 + 16\text{O/C} + \text{H/C})}{2N_a\rho D_p}[\text{OH}]t \quad (7)$$

Equation 7 allows for lifetimes to be calculated from elemental ratios (O/C and H/C), rather than from molecular weight M, which is generally poorly constrained for OA. The organic fraction of the particle is not included explicitly in eq 7, since inorganic components (water, sulfate, nitrate, etc.) are assumed to affect equally the amount of organic material within the bulk and on the surface of the particle (corresponding to the numerator and denominator of eq 7, respectively). However, if organic species are located preferentially on the surface, or if inorganic species do not affect the rate of oxidation of surface organic species, heterogeneous oxidation may be faster than

DOI: 10.1021/acs.jpca.5b06946
J. Phys. Chem. A 2015, 119, 10767−10783

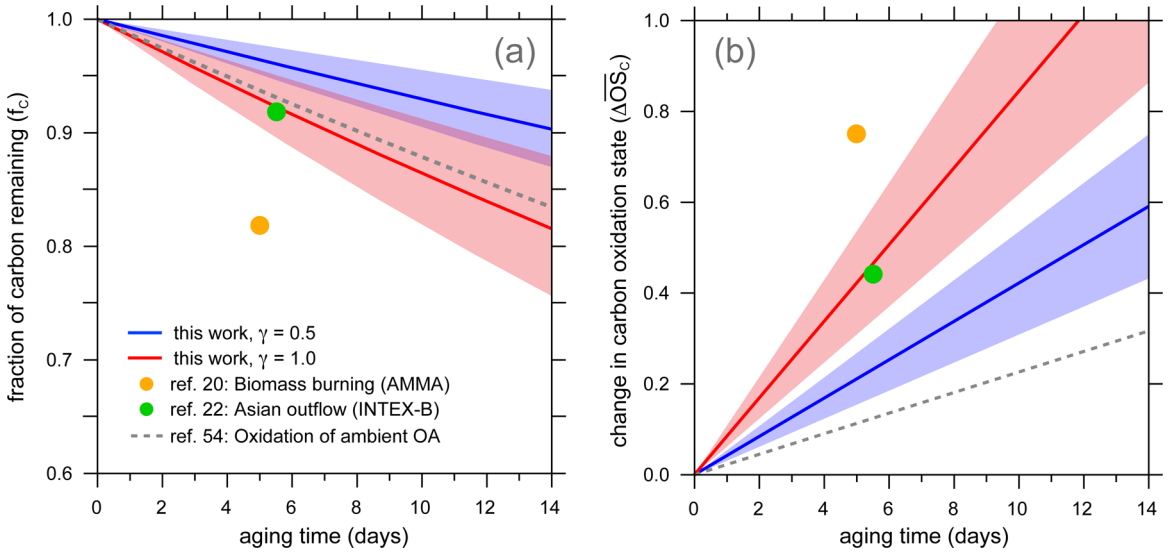

Figure 9. Predicted changes to the amount (a) and oxidation state (b) of particulate carbon in atmospheric OA as a function of particle age, using eq 7 and the fits from Figure 8. Predictions are shown for both $\gamma = 0.5$ (blue curves) and $\gamma = 1$ (red curves), with shaded regions reflecting the variability from the measurements (as in Figure 8). Also shown are results from two aircraft studies[20,22] (solid circles) in which the aging of ambient OA was inferred by measurements of plumes at very different ages, and measured changes to ambient OA subjected to high OH concentrations in the laboratory[54] (dashed line). Predicted carbon loss after one week is ~3−13%, a significant flux that is broadly in agreement with ambient measurements.

predicted by eq 7; thus, these calculations may represent a lower limit for the effects of heterogeneous oxidation. For the present calculations, typical atmospheric values are assumed: surface-area-weighted D_p = 200 nm, [OH] = 1.5 × 10^6 molec/cm^3, O/C = 0.8, H/C = 1.5, and ρ = 1.5 g cm^{-3}. For the uptake coefficient γ, laboratory measurements (after correction for diffusion) vary from 0.1 to 1.0 (or even higher when secondary chemistry occurs);[25] Figure 9 shows results for an approximate average value, $\gamma = 0.5$ (blue curve), as well as for $\gamma = 1.0$ (red curve).

The changes to f_C and $\overline{OS}_C$ shown in Figure 9 indicate that heterogeneous oxidation can have a substantial influence on aerosol composition over the atmospheric lifetime of OA: assuming $\gamma = 0.5$, after a week of oxidation (0.06 carbon lifetimes), 5.0 ± 1.8% of the particle-phase carbon will be lost to the gas phase, and $\overline{OS}_C$ of the OA will increase by 0.30 ± 0.08. The characteristic lifetime of particulate carbon versus volatilization is 137 d. These changes are essentially doubled if a γ of 1.0 is assumed, with a loss of 9.7 ± 3.5% of the particle-phase carbon and $\overline{OS}_C$ increase of 0.59 ± 0.16 after a week (0.12 carbon lifetimes), with a carbon lifetime versus volatilization of 69 d.

For comparison, also shown in Figure 9 are results from two aircraft-based field measurements of the changes in OA from plumes intercepted at different photochemical ages: a biomass burning plume, measured near the point of emission and again after ~5 d,[20] and Asian pollution outflow, measured at ~3 and ~8.5 d downwind of emission.[22] To our knowledge these are the only two ambient measurements of OA ensemble chemistry made over long timescales (>3 d), such that the observed chemical changes to OA are dominated by particle-phase oxidation processes rather than condensation (SOA formation). In both these studies OA mass loading (normalized to [CO], to account for dilution) is constant, whereas the degree of oxygenation of the OA (as measured by O/C or f_{44}, the fraction of AMS ion signal at m/z 44) increases; this necessarily implies a loss of organic carbon from the particle phase, which is quantified using eq 3. Changes to $\overline{OS}_C$ are determined using eq 2, with O/C determined from f_{44} using the relationship given by Canagaratna et al.[81] and H/C estimated from the average relationship H/C = 2.0−0.6 O/C.[84] (This represents a major approximation, though since f_C is only weakly dependent on hydrogen content of the OA, this leads to uncertainty in only the $\Delta\overline{OS}_C$ calculation.) Also shown are the estimated changes observed by George et al. when subjecting ambient OA to the equivalent of up to several weeks of heterogeneous oxidation,[54] with f_C and $\Delta\overline{OS}_C$ calculated in the same way as for the aircraft measurements.

Both ambient data sets provide clear evidence of OA aging that is consistent with our laboratory aging studies, with a measurable decrease in particulate organic carbon and increase in $\overline{OS}_C$ of the OA. Further, the magnitude of the changes are broadly consistent with the changes expected from heterogeneous oxidation, especially when assuming an uptake coefficient of unity (red bands in Figure 9). Predicted carbon loss is also consistent with the laboratory aging results of George et al.[54] and qualitatively with other laboratory studies that find modest decreases in OA mass over multiday timescales.[38,39,41,51] However, in the case of the biomass burning plume, the changes to the ambient OA with age are somewhat greater than predicted based on our heterogeneous oxidation experiments. This may arise from differences in heterogeneous oxidation kinetics, the detailed chemistry of heterogeneous reactions, and/or the importance of other OA aging processes; these highlight possible differences between laboratory and ambient reaction conditions, and are discussed below.

The kinetics of heterogeneous oxidation may differ between the laboratory and the atmosphere due to differences in the various parameters assumed in eq 7, such as particle size D_p and uptake coefficient γ (which can vary from compound to compound). Moreover, eq 7 assumes the particles are spherical and undergo rapid internal mixing. Nonspherical particles, with higher surface area-to-volume ratios than spherical ones, will undergo heterogeneous oxidation more rapidly than implied by

DOI: 10.1021/acs.jpca.5b06946
J. Phys. Chem. A 2015, 119, 10767−10783

eq 7. Additionally, the effects of inorganic aerosol components (water, sulfate, etc.) on the rate of heterogeneous oxidation of organic species are poorly understood at present. Further, as discussed above, highly viscous OA material can lead to diffusion limitations within the particles, affecting the oxidation kinetics. At room temperature, kinetic slowing due to diffusion limitations is likely to be more pronounced in the laboratory than in the atmosphere, due to the very short diffusive timescales (relative to oxidation timescales) in our experiments. However, diffusion limitations within ambient OA will be enhanced at the low temperatures of the upper troposphere.[91] All these uncertain effects thus point to the need for an improved understanding of OA reactivity, morphology/shape, and viscosity, to better understand how these impact the kinetics of heterogeneous oxidation.

In addition, the chemistry of heterogeneous oxidation may be different between our experiments and the real atmosphere. For example, the high oxidant levels may promote chemistry that is unimportant under lower-concentration conditions. In particular, the fate of particle-phase peroxy (RO_2) radicals is poorly understood at present: in our laboratory experiments, RO_2 chemistry is likely dominated by self-reaction (RO_2+RO_2), though in the atmosphere, bimolecular reactions with HO_2 or NO,[53] or unimolecular reactions,[92] may also compete. Thus, reaction time and oxidant concentration may not be strictly interchangeable,[46,50,77] as is assumed here.

Finally, the differences between predicted and measured changes to OA in Figure 9 may result from the importance of other aging mechanisms that occur in addition to heterogeneous oxidation. Such mechanisms include gas-phase oxidation of semivolatile species that partition to the gas phase,[24] photolysis of OA components,[93,94] and multiphase (aqueous) oxidation.[27] Gas-phase oxidation of semivolatile OA components is unlikely to be a major aging mechanism after several days, given that only low-volatility species are likely to remain in the particle phase after substantial dilution and oxidation. Recent work[95,96] has shown that the photolysis of condensed-phase species can lead to the loss of OA, but this may also be most pronounced for "fresh" SOA.[96] Aqueous-phase oxidation has received attention mostly as a potential OA source, but it can also lead to the chemical degradation of organic species[97] and so may contribute to observed carbon loss over timescales of several days.

Despite the above uncertainties, the general agreement between ambient and laboratory measurements of OA aging suggests that heterogeneous oxidation is indeed an important process affecting the amount and properties of atmospheric OA over multiday timescales. The measured changes to the amount and oxidation state of particle-phase carbon (as described by f_C and $\Delta\overline{OS}_C$, respectively) with oxidation (expressed in carbon lifetimes)—shown as the shaded areas in Figure 8—also provides a simple, straightforward approach for inclusion of this process within CTMs.

More generally, this work points to the importance of atmospheric oxidation as a sink of OA. Previous calculations and modeling studies have shown that heterogeneous oxidation has the potential to decrease OA mass,[11,67,68,98,99] but all used simple parametrizations of carbon loss that were not directly based on laboratory measurements of OA aging; as a result the predicted timescales of OA mass loss vary dramatically from study to study (ranging from days[98] to months[99]), depending on the assumptions made about the rate of degradation. The present work a provides a new laboratory-based estimate of this loss process and suggests that heterogeneous oxidation leads to the loss of a substantial fraction (~3−13%) of particulate organic carbon during OA's atmospheric lifetime (assumed to be one week). This loss of OA carbon will not be uniform throughout the atmosphere, but instead will depend on depositional lifetimes, which vary with altitude and latitude.[23] Further, as discussed above, total carbon loss from all OA aging processes may be somewhat greater than predicted here, given the faster rate of carbon loss inferred from ambient measurements (Figure 9).

Recent top-down estimates indicate a global OA production rate of ~150 Tg C/yr (with an uncertainty on the order of ±80%);[100,101] combined with the present estimate of carbon loss, this implies a global flux of ~11 Tg C/yr (full uncertainty range of 1−35 Tg C/yr) from the particle phase to the gas phase as a result of heterogeneous oxidation. This is smaller than a previous estimate based on a much more aggressive heterogeneous oxidation scheme,[98] but nonetheless it still represents a substantial sink of particulate carbon. This production of volatile oxidized carbon (e.g., CO, CO_2, and OVOCs) is a small fraction (~1%) of total secondary sources[16] but may still have an impact on atmospheric composition (e.g., OVOC budgets) if emitted in remote areas such as the free troposphere. Any such impacts will also depend on the molecular identities of the volatile species produced, which were not measured in this work. Several studies have examined the formation of these small oxidation products,[41,43,64,66] but the yields of individual species, and even the branching between inorganic (CO/CO_2) and organic (OVOC) products, remain poorly constrained. Thus, at present it is difficult to estimate the impact of this carbon mass loss on gas-phase species in the atmosphere.

CONCLUSIONS

In this work we have compiled and reanalyzed a number of our previous measurements of the heterogeneous oxidation of single-component aerosol particles. Measurements of the change in the amount and oxidation state of particulate organic carbon were presented as a function of a new metric for heterogeneous oxidation kinetics, the number of carbon oxidation lifetimes. In all systems studied, heterogeneous oxidation leads to the loss of particle-phase organic carbon to the gas phase, as a result of C−C bond scission (fragmentation) reactions followed by volatilization; meanwhile, the organic carbon remaining in the particle phase becomes increasingly oxidized, likely from both functionalization and fragmentation reactions. The actual rate of this increase, as described by $\Delta\overline{OS}_C$ versus carbon lifetimes (a measure of the changes to the oxidation state of the carbon atom(s) being oxidized), varies substantially among the different chemical systems studied, presumably due to differences in chemical mechanisms. For low-volatility species that include no C═C double bonds, $\Delta\overline{OS}_C$ per carbon atom reacted is 4.9 ± 1.3. The loss of carbon, as described by f_C versus carbon lifetimes (a measure of the likelihood that a carbon atom will be lost from the particle for each carbon atom oxidized), is likely driven by "activated" alkoxy radicals, which undergo efficient fragmentation. Carbon loss shows less variability than the increase in $\overline{OS}_C$, with an average loss of 0.6 atoms per carbon atom reacted for most systems studied.

From these results we have estimated the effects of heterogeneous oxidation on the oxidation state and amount

DOI: 10.1021/acs.jpca.5b06946
J. Phys. Chem. A 2015, 119, 10767−10783

of particle-phase carbon as a function of photochemical age. Changes to both quantities are predicted to be significant over multiday timescales; most importantly, a loss of 3−13% of particulate carbon after a week of aging is predicted. The general agreement with ambient measurements of OA aging over long timescales gives us some confidence in these predictions and suggests that heterogeneous oxidation can indeed have a substantial influence on the loadings and properties of atmospheric OA. At the same time, numerous uncertainties remain that limit our ability to quantitatively and accurately estimate the atmospheric impacts of heterogeneous oxidation. These include the role of OA physical properties (shape, morphology, mixing state, and viscosity) and chemical properties (chemical structure of the organic species) on the heterogeneous oxidation kinetics; the detailed chemistry of radicals (OH, RO, RO_2, etc.), at the air-surface interface and within the bulk condensed phase; and the importance of other aging processes (e.g., photolysis, aqueous-phase chemistry) relative to heterogeneous oxidation. All of these represent important target areas for future laboratory research. Additional ambient measurements of OA aging, based on (pseudo-) Lagrangian studies of plumes over several days, would also be exceedingly useful for better constraining the rates and effects of oxidative aging of atmospheric OA particles.

The experiments and analysis in this work focus on the ensemble chemical properties of OA. The major quantities examined—loading, average chemical composition, and reaction kinetics—are characterized in terms of the constituent organic carbon, rather than the individual molecular components, of OA. This provides a complete and quantitative description of the entire organic mixture, which more detailed molecular-level approaches often cannot provide. Such speciated measurements are critically important for understanding the chemical mechanisms that underlie OA formation and aging; in fact, measurements of molecular species are used in the present study to constrain the oxidation kinetics. However, as we have shown here, much simpler ensemble descriptions can still provide considerable information about OA loading, composition, and reactivity. Because of their relative simplicity, such ensemble approaches are generally more directly useful for inclusion within CTMs than molecular-based descriptions; they also tend to be more compatible with current models, given that most models already simulate OA as an ensemble. Additionally, ensemble approaches can extend well beyond descriptions of OA chemistry in terms of simple average properties, the focus of this work. For example, ensemble quantities can be expressed as complex distributions rather than averages[10,89] and can be related to key physicochemical properties of OA (such as index of refraction, hygroscopicity, and volatility).[13,17,62,63] Further development of such approaches is likely to lead to improved chemical frameworks and models for predicting the loading, composition, and ultimate impacts of atmospheric OA.

AUTHOR INFORMATION

Corresponding Author

*E-mail: jhkroll@mit.edu.

Notes

The authors declare no competing financial interest.

Biographies

Jesse Kroll received an A.B. in Chemistry and Earth and Planetary Sciences and a Ph.D. in Chemistry from Harvard University. Following a postdoctoral appointment at Caltech and a Senior Scientist position at Aerodyne Research, he joined the Departments of Civil and Environmental Engineering and Chemical Engineering at MIT, where he is now an Associate Professor. His research group studies the lifecycle of atmospheric organic carbon in the Earth's atmosphere, with a major focus on laboratory studies of the formation and oxidative aging of organic aerosol.

Christopher Lim is a graduate student in Civil and Environmental Engineering at the Massachusetts Institute of Technology. He received a B.S. in Chemistry from the University of California, Berkeley, with a minor course of study in Energy and Resources. Prior to arriving at MIT, he worked as a research associate for Nanosys, Inc. on quantum dot technology for displays. His current research focus is on the heterogeneous oxidation of organic aerosol and how phase and morphology impact the kinetics of oxidation.

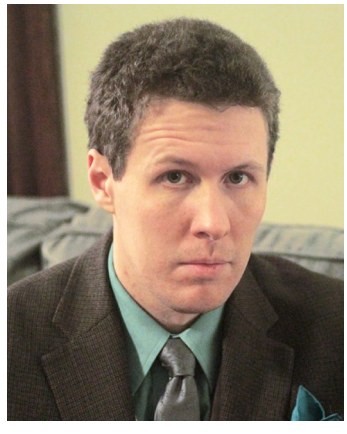

DOI: 10.1021/acs.jpca.5b06946
J. Phys. Chem. A 2015, 119, 10767−10783

Sean Kessler is a postdoctoral researcher in the Civil and Environmental Engineering Department at the Massachusetts Institute of Technology. He holds a B.S. in Chemical Engineering from Lehigh University and a Ph.D. in Chemical Engineering from the Massachusetts Institute of Technology, where he was named a member of the Martin Family Society of Fellows for Sustainability. His current research focuses on the application of inverse methods for development of models pertaining both to complex atmospheric systems and to the chemistry of nuclear materials.

Kevin Wilson is a Staff Scientist and Deputy Division Director in the Chemical Sciences Division at Lawrence Berkeley National Laboratory. He received a B.A. in Chemistry from Willamette University, an M.A. in Humanities from St. John's College, and a Ph.D. in Chemistry from the University of California, Berkeley, and carried out postdoctoral research at Los Alamos National Laboratory. His research group is interested in water uptake and heterogeneous reactions at aqueous and organic aerosol interfaces.

■ ACKNOWLEDGMENTS

This work was supported by the National Science Foundation under Grant Nos. AGS-1056225 and CHE-1307664. K.R.W. is supported by the Department of Energy, Office of Science Early Career Research Program and by the Director, Office of Energy Research, Office of Basic Energy Sciences, Chemical Sciences Division of the U.S. Department of Energy under Contract No. DE-AC02-05CH11231. The authors are grateful to the numerous colleagues involved in the original experiments, including J. Smith, T. Nah, D. Che, M. N. Chan, K. Daumit, C.-l. Liu, H. Zhang, M. Ahmed, C. Cappa, A. Goldstein, and S. Leone; J.H.K. and K.R.W. would especially like to acknowledge D. Worsnop for initiating and fostering the collaboration that led to this work.

■ REFERENCES

(1) Kanakidou, M.; Seinfeld, J. H.; Pandis, S. N.; Barnes, I.; Dentener, F.; Facchini, C.; van Dingenen, R.; Ervens, B.; Nenes, A.; Nielsen, C. J.; et al. Organic Aerosol and Global Climate Modelling: a Review. *Atmos. Chem. Phys.* **2005**, *5*, 1053−1123.

(2) Zhang, Q.; Jimenez, J. L.; Canagaratna, M. R.; Allan, J. D.; Coe, H.; Ulbrich, I.; Alfarra, M. R.; Takami, A.; Middlebrook, A. M.; Sun, Y. L.; et al. Ubiquity and Dominance of Oxygenated Species in Organic Aerosols in Anthropogenically-Influenced Northern Hemisphere Midlatitudes. *Geophys. Res. Lett.* **2007**, *34*, L13801.

(3) Aumont, B.; Szopa, S.; Madronich, S. Modelling the Evolution of Organic Carbon During Its Gas-Phase Tropospheric Oxidation: Development of an Explicit Model Based on a Self Generating Approach. *Atmos. Chem. Phys.* **2005**, *5*, 2497−2517.

(4) Kroll, J. H.; Donahue, N. M.; Jimenez, J. L.; Kessler, S. H.; Canagaratna, M. R.; Wilson, K. R.; Altieri, K. E.; Mazzoleni, L. R.; Wozniak, A. S.; Bluhm, H.; et al. Carbon Oxidation State as a Metric for Describing the Chemistry of Atmospheric Organic Aerosol. *Nat. Chem.* **2011**, *3*, 133−139.

(5) Yatavelli, R.; Lopez-Hilfiker, F.; Wargo, J. D.; Kimmel, J. R.; Cubison, M. J.; Bertram, T. H.; Jimenez, J. L.; Gonin, M.; Worsnop, D. R.; Thornton, J. A. A Chemical Ionization High-Resolution Time-of-Flight Mass Spectrometer Coupled to a Micro Orifice Volatilization Impactor (MOVI-HRToF-CIMS) for Analysis of Gas and Particle-Phase Organic Species. *Aerosol Sci. Technol.* **2012**, *46*, 1313−1327.

(6) Jokinen, T.; Sipila, M.; Junninen, H.; Ehn, M.; Lönn, G.; Hakala, J.; Petäjä, T.; Mauldin, R. L., III; Kulmala, M.; Worsnop, D. R. Atmospheric Sulphuric Acid and Neutral Cluster Measurements Using CI-APi-TOF. *Atmos. Chem. Phys.* **2012**, *12*, 4117−4125.

(7) Crounse, J. D.; Paulot, F.; Kjaergaard, H. G.; Wennberg, P. O. Peroxy Radical Isomerization in the Oxidation of Isoprene. *Phys. Chem. Chem. Phys.* **2011**, *13*, 13607.

(8) Pankow, J. F.; Barsanti, K. C. The Carbon Number-Polarity Grid: a Means to Manage the Complexity of the Mix of Organic Compounds When Modeling Atmospheric Organic Particulate Matter. *Atmos. Environ.* **2009**, *43*, 2829−2835.

(9) Heald, C. L.; Kroll, J. H.; Jimenez, J. L.; Docherty, K. S.; Decarlo, P. F.; Aiken, A. C.; Chen, Q.; Martin, S. T.; Farmer, D. K.; Artaxo, P. A Simplified Description of the Evolution of Organic Aerosol Composition in the Atmosphere. *Geophys. Res. Lett.* **2010**, *37*, L08803.

(10) Donahue, N. M.; Kroll, J. H.; Pandis, S. N.; Robinson, A. L. A Two-Dimensional Volatility Basis Set − Part 2: Diagnostics of Organic-Aerosol Evolution. *Atmos. Chem. Phys.* **2012**, *12*, 615−634.

(11) Cappa, C. D.; Wilson, K. R. Multi-Generation Gas-Phase Oxidation, Equilibrium Partitioning, and the Formation and Evolution of Secondary Organic Aerosol. *Atmos. Chem. Phys.* **2012**, *12*, 9505−9528.

(12) Wei, Y.; Cao, T.; Thompson, J. E. The Chemical Evolution & Physical Properties of Organic Aerosol: a Molecular Structure Based Approach. *Atmos. Environ.* **2012**, *62*, 199−207.

(13) Daumit, K. E.; Kessler, S. H.; Kroll, J. H. Average Chemical Properties and Potential Formation Pathways of Highly Oxidized Organic Aerosol. *Faraday Discuss.* **2013**, *165*, 181−202.

(14) Shiraiwa, M.; Berkemeier, T.; Schilling-Fahnestock, K. A.; Seinfeld, J. H.; Pöschl, U. Molecular Corridors and Kinetic Regimes in the Multiphase Chemical Evolution of Secondary Organic Aerosol. *Atmos. Chem. Phys.* **2014**, *14*, 8323−8341.

(15) Kroll, J. H.; Seinfeld, J. H. Chemistry of Secondary Organic Aerosol: Formation and Evolution of Low-Volatility Organics in the Atmosphere. *Atmos. Environ.* **2008**, *42*, 3593−3624.

(16) Hallquist, M.; Wenger, J. C.; Baltensperger, U.; Rudich, Y.; Simpson, D.; Claeys, M.; Dommen, J.; Donahue, N. M.; George, C.; Goldstein, A. H.; et al. The Formation, Properties and Impact of Secondary Organic Aerosol: Current and Emerging Issues. *Atmos. Chem. Phys.* **2009**, *9*, 5155−5236.

(17) Jimenez, J. L.; Canagaratna, M. R.; Donahue, N. M.; Prevot, A. S. H.; Zhang, Q.; Kroll, J. H.; Decarlo, P. F.; Allan, J. D.; Coe, H.; Ng, N. L.; et al. Evolution of Organic Aerosols in the Atmosphere. *Science* **2009**, *326*, 1525−1529.

(18) Rudich, Y.; Donahue, N. M.; Mentel, T. F. Aging of Organic Aerosol: Bridging the Gap Between Laboratory and Field Studies. *Annu. Rev. Phys. Chem.* **2007**, *58*, 321−352.

(19) Decarlo, P. F.; Ulbrich, I. M.; Crounse, J.; de Foy, B.; Dunlea, E. J.; Aiken, A. C.; Knapp, D.; Weinheimer, A. J.; Campos, T.; Wennberg, P. O.; et al. Investigation of the Sources and Processing of Organic Aerosol Over the Central Mexican Plateau From Aircraft Measurements During MILAGRO. *Atmos. Chem. Phys.* **2010**, *10*, 5257−5280.

(20) Capes, G.; Johnson, B.; McFiggans, G.; Williams, P. I.; Haywood, J.; Coe, H. Aging of Biomass Burning Aerosols Over West Africa: Aircraft Measurements of Chemical Composition, Microphysical Properties, and Emission Ratios. *J. Geophys. Res.* **2008**, *113*, D00C15.

(21) Decarlo, P. F.; Dunlea, E. J.; Kimmel, J. R.; Aiken, A. C.; Sueper, D.; Crounse, J.; Wennberg, P. O.; Emmons, L.; Shinozuka, Y.; Clarke, A.; et al. Fast Airborne Aerosol Size and Chemistry Measurements

DOI: 10.1021/acs.jpca.5b06946
J. Phys. Chem. A 2015, 119, 10767−10783

with the High Resolution Aerosol Mass Spectrometer During the MILAGRO Campaign. *Atmos. Chem. Phys.* **2008**, *8*, 4027−4048.
(22) Dunlea, E. J.; Decarlo, P. F.; Aiken, A. C.; Kimmel, J. R.; Peltier, R. E.; Weber, R. J.; Tomlinson, J.; Collins, D. R.; Shinozuka, Y.; McNaughton, C. S. Evolution of Asian Aerosols During Transpacific Transport in INTEX-B. *Atmos. Chem. Phys.* **2009**, *9*, 7257−7287.
(23) Balkanski, Y. J.; Jacob, D. J.; Gardner, G. M.; Graustein, W. C.; Turekian, K. K. Transport and Residence Times of Tropospheric Aerosols Inferred From a Global Three-Dimensional Simulation of ^{210}Pb. *J. Geophys. Res.* **1993**, *98*, 20573−20586.
(24) Robinson, A. L.; Donahue, N. M.; Shrivastava, M. K.; Weitkamp, E. A.; Sage, A. M.; Grieshop, A. P.; Lane, T. E.; Pierce, J. R.; Pandis, S. N. Rethinking Organic Aerosols: Semivolatile Emissions and Photochemical Aging. *Science* **2007**, *315*, 1259−1262.
(25) George, I. J.; Abbatt, J. P. D. Heterogeneous Oxidation of Atmospheric Aerosol Particles by Gas-Phase Radicals. *Nat. Chem.* **2010**, *2*, 713−722.
(26) Robinson, A. L.; Donahue, N. M.; Rogge, W. F. Photochemical Oxidation and Changes in Molecular Composition of Organic Aerosol in the Regional Context. *J. Geophys. Res.* **2006**, *111*, D03302.
(27) Ervens, B.; Turpin, B. J.; Weber, R. J. Secondary Organic Aerosol Formation in Cloud Droplets and Aqueous Particles (aqSOA): a Review of Laboratory, Field and Model Studies. *Atmos. Chem. Phys.* **2011**, *11*, 11069−11102.
(28) Decesari, S.; Mircea, M.; Cavalli, F.; Fuzzi, S.; Moretti, F.; Tagliavini, E.; Facchini, M. C. Source Attribution of Water-Soluble Organic Aerosol by Nuclear Magnetic Resonance Spectroscopy. *Environ. Sci. Technol.* **2007**, *41*, 2479−2484.
(29) Mysak, E. R.; Smith, J. D.; Ashby, P. D.; Newberg, J. T.; Wilson, K. R.; Bluhm, H. Competitive Reaction Pathways for Functionalization and Volatilization in the Heterogeneous Oxidation of Coronene Thin Films by Hydroxyl Radicals and Ozone. *Phys. Chem. Chem. Phys.* **2011**, *13*, 7554.
(30) Moffet, R. C.; Henn, T.; Laskin, A.; Gilles, M. K. Automated Chemical Analysis of Internally Mixed Aerosol Particles Using X-Ray Spectromicroscopy at the Carbon K-Edge. *Anal. Chem.* **2010**, *82*, 7906−7914.
(31) Atkinson, R. Rate Constants for the Atmospheric Reactions of Alkoxy Radicals: an Updated Estimation Method. *Atmos. Environ.* **2007**, *41*, 8468−8485.
(32) Calvert, J. G.; Atkinson, R.; Kerr, J. A.; Madronich, S.; Moortgat, G. K.; Wallington, T. J.; Yarwood, G. *The Mechanisms of Atmospheric Oxidation of the Alkenes;* Oxford University Press: New York, 2010.
(33) Epstein, S. A.; Tapavicza, E.; Furche, F.; Nizkorodov, S. A. Direct Photolysis of Carbonyl Compounds Dissolved in Cloud and Fog Droplets. *Atmos. Chem. Phys.* **2013**, *13*, 9461−9477.
(34) Crounse, J. D.; Knap, H. C.; Ørnsø, K. B.; Jørgensen, S.; Paulot, F.; Kjaergaard, H. G.; Wennberg, P. O. Atmospheric Fate of Methacrolein. 1. Peroxy Radical Isomerization Following Addition of OH and O_2. *J. Phys. Chem. A* **2012**, *116*, 5756−5762.
(35) Kjaergaard, H. G.; Knap, H. C.; Ørnsø, K. B.; Jørgensen, S.; Crounse, J. D.; Paulot, F.; Wennberg, P. O. Atmospheric Fate of Methacrolein. 2. Formation of Lactone and Implications for Organic Aerosol Production. *J. Phys. Chem. A* **2012**, *116*, 5763−5768.
(36) Bertram, A. K.; Ivanov, A. V.; Hunter, M.; Molina, L. T.; Molina, M. J. The Reaction Probability of OH on Organic Surfaces of Tropospheric Interest. *J. Phys. Chem. A* **2001**, *105*, 9415−9421.
(37) Moise, T.; Rudich, Y. Uptake of Cl and Br by Organic Surfaces—a Perspective on Organic Aerosols Processing by Tropospheric Oxidants. *Geophys. Res. Lett.* **2001**, *28*, 4083.
(38) Knopf, D. A.; Mak, J.; Gross, S.; Bertram, A. K. Does Atmospheric Processing of Saturated Hydrocarbon Surfaces by NO_3 Lead to Volatilization? *Geophys. Res. Lett.* **2006**, *33*, L17816.
(39) Hearn, J. D.; Renbaum, L. H.; Wang, X.; Smith, G. D. Kinetics and Products From Reaction of Cl Radicals with Dioctyl Sebacate (DOS) Particles in O_2: A Model for Radical-Initiated Oxidation of Organic Aerosols. *Phys. Chem. Chem. Phys.* **2007**, *9*, 4803.
(40) McNeill, V. F.; Wolfe, G. M.; Thornton, J. A. The Oxidation of Oleate in Submicron Aqueous Salt Aerosols: Evidence of a Surface Process. *J. Phys. Chem. A* **2007**, *111*, 1073−1083.
(41) McNeill, V. F.; Yatavelli, R.; Thornton, J. A.; Stipe, C. B.; Landgrebe, O. Heterogeneous OH Oxidation of Palmitic Acid in Single Component and Internally Mixed Aerosol Particles: Vaporization and the Role of Particle Phase. *Atmos. Chem. Phys.* **2008**, *8*, 5465−5476.
(42) Renbaum, L. H.; Smith, G. D. The Importance of Phase in the Radical-Initiated Oxidation of Model Organic Aerosols: Reactions of Solid and Liquid Brassidic Acid Particles. *Phys. Chem. Chem. Phys.* **2009**, *11*, 2441.
(43) Slade, J. H.; Knopf, D. A. Heterogeneous OH Oxidation of Biomass Burning Organic Aerosol Surrogate Compounds: Assessment of Volatilisation Products and the Role of OH Concentration on the Reactive Uptake Kinetics. *Phys. Chem. Chem. Phys.* **2013**, *15*, 5898.
(44) Slade, J. H.; Knopf, D. A. Multiphase OH Oxidation Kinetics of Organic Aerosol: the Role of Particle Phase State and Relative Humidity. *Geophys. Res. Lett.* **2014**, *41*, 5297−5306.
(45) Zhao, Z.; Husainy, S.; Stoudemayer, C. T.; Smith, G. D. Reactive Uptake of NO_3 Radicals by Unsaturated Fatty Acid Particles. *Phys. Chem. Chem. Phys.* **2011**, *13*, 17809.
(46) Renbaum, L. H.; Smith, G. D. Artifacts in Measuring Aerosol Uptake Kinetics: the Roles of Time, Concentration and Adsorption. *Atmos. Chem. Phys.* **2011**, *11*, 6881−6893.
(47) Knopf, D. A.; Forrester, S. M.; Slade, J. H. Heterogeneous Oxidation Kinetics of Organic Biomass Burning Aerosol Surrogates by O_3, NO_2, N_2O_5, And NO_3. *Phys. Chem. Chem. Phys.* **2011**, *13*, 21050.
(48) Lambe, A. T.; Zhang, J.; Sage, A. M.; Donahue, N. M. Controlled OH Radical Production via Ozone-Alkene Reactions for Use in Aerosol Aging Studies. *Environ. Sci. Technol.* **2007**, *41*, 2357−2363.
(49) Isaacman, G.; Chan, A. W. H.; Nah, T.; Worton, D. R.; Ruehl, C. R.; Wilson, K. R.; Goldstein, A. H. Heterogeneous OH Oxidation of Motor Oil Particles Causes Selective Depletion of Branched and Less Cyclic Hydrocarbons. *Environ. Sci. Technol.* **2012**, *46*, 10632−10640.
(50) Liu, C.-L.; Smith, J. D.; Che, D. L.; Ahmed, M.; Leone, S. R.; Wilson, K. R. The Direct Observation of Secondary Radical Chain Chemistry in the Heterogeneous Reaction of Chlorine Atoms with Submicron Squalane Droplets. *Phys. Chem. Chem. Phys.* **2011**, *13*, 8993.
(51) George, I. J.; Vlasenko, A.; Slowik, J. G.; Broekhuizen, K.; Abbatt, J. Heterogeneous Oxidation of Saturated Organic Aerosols by Hydroxyl Radicals: Uptake Kinetics, Condensed-Phase Products, and Particle Size Change. *Atmos. Chem. Phys.* **2007**, *7*, 4187−4201.
(52) Docherty, K. S.; Ziemann, P. J. Reaction of Oleic Acid Particles with NO_3 Radicals: Products, Mechanism, and Implications for Radical-Initiated Organic Aerosol Oxidation. *J. Phys. Chem. A* **2006**, *110*, 3567−3577.
(53) Renbaum, L. H.; Smith, G. D. Organic Nitrate Formation in the Radical-Initiated Oxidation of Model Aerosol Particles in the Presence of NO_X. *Phys. Chem. Chem. Phys.* **2009**, *11*, 8040.
(54) George, I. J.; Slowik, J.; Abbatt, J. P. D. Chemical Aging of Ambient Organic Aerosol From Heterogeneous Reaction with Hydroxyl Radicals. *Geophys. Res. Lett.* **2008**, *35*, L13811.
(55) George, I. J.; Abbatt, J. P. D. Chemical Evolution of Secondary Organic Aerosol From OH-Initiated Heterogeneous Oxidation. *Atmos. Chem. Phys.* **2010**, *10*, 5551−5563.
(56) Nah, T.; Kessler, S. H.; Daumit, K. E.; Kroll, J. H.; Leone, S. R.; Wilson, K. R. Influence of Molecular Structure and Chemical Functionality on the Heterogeneous OH-Initiated Oxidation of Unsaturated Organic Particles. *J. Phys. Chem. A* **2014**, *118*, 4106−4119.
(57) Ruehl, C. R.; Nah, T.; Isaacman, G.; Worton, D. R.; Chan, A. W. H.; Kolesar, K. R.; Cappa, C. D.; Goldstein, A. H.; Wilson, K. R. The Influence of Molecular Structure and Aerosol Phase on the Heterogeneous Oxidation of Normal and Branched Alkanes by OH. *J. Phys. Chem. A* **2013**, *117*, 3990−4000.

DOI: 10.1021/acs.jpca.5b06946
J. Phys. Chem. A 2015, 119, 10767−10783

(58) Zhang, H.; Ruehl, C. R.; Chan, A. W. H.; Nah, T.; Worton, D. R.; Isaacman, G.; Goldstein, A. H.; Wilson, K. R. OH-Initiated Heterogeneous Oxidation of Cholestane: a Model System for Understanding the Photochemical Aging of Cyclic Alkane Aerosols. *J. Phys. Chem. A* **2013**, *117*, 12449−12458.
(59) Zuberi, B.; Johnson, K. S.; Aleks, G. K.; Molina, L. T.; Molina, M. J. Hydrophilic Properties of Aged Soot. *Geophys. Res. Lett.* **2005**, *32*, L01807.
(60) Petters, M. D.; Prenni, A. J.; Kreidenweis, S. M.; DeMott, P. J.; Matsunaga, A.; Lim, Y. B.; Ziemann, P. J. Chemical Aging and the Hydrophobic-to-Hydrophilic Conversion of Carbonaceous Aerosol. *Geophys. Res. Lett.* **2006**, *33*, L24806.
(61) George, I. J.; Chang, R. Y. W.; Danov, V.; Vlasenko, A.; Abbatt, J. P. D. Modification of Cloud Condensation Nucleus Activity of Organic Aerosols by Hydroxyl Radical Heterogeneous Oxidation. *Atmos. Environ.* **2009**, *43*, 5038−5045.
(62) Cappa, C. D.; Che, D. L.; Kessler, S. H.; Kroll, J. H.; Wilson, K. R. Variations in Organic Aerosol Optical and Hygroscopic Properties Upon Heterogeneous OH Oxidation. *J. Geophys. Res.* **2011**, *116*, D15204.
(63) Harmon, C. W.; Ruehl, C. R.; Cappa, C. D.; Wilson, K. R. A Statistical Description of the Evolution of Cloud Condensation Nuclei Activity During the Heterogeneous Oxidation of Squalane and Bis(2-Ethylhexyl) Sebacate Aerosol by Hydroxyl Radicals. *Phys. Chem. Chem. Phys.* **2013**, *15*, 9679.
(64) Molina, M. J.; Ivanov, A. V.; Trakhtenberg, S.; Molina, L. T. Atmospheric Evolution of Organic Aerosol. *Geophys. Res. Lett.* **2004**, *31*, L22104.
(65) Eliason, T. L.; Gilman, J. B.; Vaida, V. Oxidation of Organic Films Relevant to Atmospheric Aerosols. *Atmos. Environ.* **2004**, *38*, 1367−1378.
(66) Vlasenko, A.; George, I. J.; Abbatt, J. P. D. Formation of Volatile Organic Compounds in the Heterogeneous Oxidation of Condensed-Phase Organic Films by Gas-Phase OH. *J. Phys. Chem. A* **2008**, *112*, 1552−1560.
(67) Heald, C. L.; Coe, H.; Jimenez, J. L.; Weber, R. J.; Bahreini, R.; Middlebrook, A. M.; Russell, L. M.; Jolleys, M.; Fu, T. M.; Allan, J. D.; et al. Exploring the Vertical Profile of Atmospheric Organic Aerosol: Comparing 17 Aircraft Field Campaigns with a Global Model. *Atmos. Chem. Phys.* **2011**, *11*, 12673−12696.
(68) Murphy, B. N.; Donahue, N. M.; Fountoukis, C.; Dall'Osto, M.; O'Dowd, C.; Kiendler-Scharr, A.; Pandis, S. N. Functionalization and Fragmentation During Ambient Organic Aerosol Aging: Application of the 2-D Volatility Basis Set to Field Studies. *Atmos. Chem. Phys.* **2012**, *12*, 10797−10816.
(69) Kroll, J. H.; Smith, J. D.; Worsnop, D. R.; Wilson, K. R. Characterisation of Lightly Oxidised Organic Aerosol Formed From the Photochemical Aging of Diesel Exhaust Particles. *Environ. Chem.* **2012**, *9*, 211.
(70) Kessler, S. H.; Nah, T.; Daumit, K. E.; Smith, J. D.; Leone, S. R.; Kolb, C. E.; Worsnop, D. R.; Wilson, K. R.; Kroll, J. H. OH-Initiated Heterogeneous Aging of Highly Oxidized Organic Aerosol. *J. Phys. Chem. A* **2012**, *116*, 6358−6365.
(71) Browne, E. C.; Franklin, J. P.; Canagaratna, M. R.; Massoli, P.; Kirchstetter, T. W.; Worsnop, D. R.; Wilson, K. R.; Kroll, J. H. Changes to the Chemical Composition of Soot From Heterogeneous Oxidation Reactions. *J. Phys. Chem. A* **2015**, *119*, 1154−1163.
(72) Smith, J. D.; Kroll, J. H.; Cappa, C. D.; Che, D. L.; Liu, C. L.; Ahmed, M.; Leone, S. R.; Worsnop, D. R.; Wilson, K. R. The Heterogeneous Reaction of Hydroxyl Radicals with Sub-Micron Squalane Particles: a Model System for Understanding the Oxidative Aging of Ambient Aerosols. *Atmos. Chem. Phys. Discuss.* **2009**, *9*, 3945−3981.
(73) Kroll, J. H.; Smith, J. D.; Che, D. L.; Kessler, S. H.; Worsnop, D. R.; Wilson, K. R. Measurement of Fragmentation and Functionalization Pathways in the Heterogeneous Oxidation of Oxidized Organic Aerosol. *Phys. Chem. Chem. Phys.* **2009**, *11*, 8005.
(74) Kessler, S. H.; Smith, J. D.; Che, D. L.; Worsnop, D. R.; Wilson, K. R.; Kroll, J. H. Chemical Sinks of Organic Aerosol: Kinetics and Products of the Heterogeneous Oxidation of Erythritol and Levoglucosan. *Environ. Sci. Technol.* **2010**, *44*, 7005−7010.
(75) Nah, T.; Kessler, S. H.; Daumit, K. E.; Kroll, J. H.; Leone, S. R.; Wilson, K. R. OH-Initiated Oxidation of Sub-Micron Unsaturated Fatty Acid Particles. *Phys. Chem. Chem. Phys.* **2013**, *15*, 18649.
(76) Chan, M. N.; Zhang, H.; Goldstein, A. H.; Wilson, K. R. Role of Water and Phase in the Heterogeneous Oxidation of Solid and Aqueous Succinic Acid Aerosol by Hydroxyl Radicals. *J. Phys. Chem. C* **2014**, *118*, 28978−28992.
(77) Che, D. L.; Smith, J. D.; Leone, S. R.; Ahmed, M.; Wilson, K. R. Quantifying the Reactive Uptake of OH by Organic Aerosols in a Continuous Flow Stirred Tank Reactor. *Phys. Chem. Chem. Phys.* **2009**, *11*, 7885−7895.
(78) DeCarlo, P. F.; Kimmel, J. R.; Trimborn, A.; Northway, M. J.; Jayne, J. T.; Aiken, A. C.; Gonin, M.; Fuhrer, K.; Horvath, T.; Docherty, K. S.; et al. Field-Deployable, High-Resolution, Time-of-Flight Aerosol Mass Spectrometer. *Anal. Chem.* **2006**, *78*, 8281−8289.
(79) Aiken, A. C.; DeCarlo, P. F.; Jimenez, J. L. Elemental Analysis of Organic Species with Electron Ionization High-Resolution Mass Spectrometry. *Anal. Chem.* **2007**, *79*, 8350−8358.
(80) Aiken, A. C.; DeCarlo, P. F.; Kroll, J. H.; Worsnop, D. R.; Huffman, J. A.; Docherty, K. S.; Ulbrich, I. M.; Mohr, C.; Kimmel, J. R.; Sueper, D.; et al. O/C and OM/OC Ratios of Primary, Secondary, and Ambient Organic Aerosols with High-Resolution Time-of-Flight Aerosol Mass Spectrometry. *Environ. Sci. Technol.* **2008**, *42*, 4478−4485.
(81) Canagaratna, M. R.; Jimenez, J. L.; Kroll, J. H.; Chen, Q.; Kessler, S. H.; Massoli, P.; Hildebrandt Ruiz, L.; Fortner, E.; Williams, L. R.; Wilson, K. R.; et al. Elemental Ratio Measurements of Organic Compounds Using Aerosol Mass Spectrometry: Characterization, Improved Calibration, and Implications. *Atmos. Chem. Phys.* **2015**, *15*, 253−272.
(82) DeCarlo, P. F.; Slowik, J. G.; Worsnop, D. R.; Davidovits, P.; Jimenez, J. L. Particle Morphology and Density Characterization by Combined Mobility and Aerodynamic Diameter Measurements. Part 1: Theory. *Aerosol Sci. Technol.* **2004**, *38*, 1185−1205.
(83) Ng, N. L.; Canagaratna, M. R.; Jimenez, J. L.; Chhabra, P. S.; Seinfeld, J. H.; Worsnop, D. R. Changes in Organic Aerosol Composition with Aging Inferred From Aerosol Mass Spectra. *Atmos. Chem. Phys.* **2011**, *11*, 6465−6474.
(84) Chen, Q.; Heald, C. L.; Jimenez, J. L.; Canagaratna, M. R.; Zhang, Q.; He, L.-Y.; Huang, X.-F.; Campuzano-Jost, P.; Palm, B. B.; Poulain, L.; et al. Elemental Composition of Organic Aerosol: the Gap Between Ambient and Laboratory Measurements. *Geophys. Res. Lett.* **2015**, *42*, 4182−4189.
(85) Claeys, M.; Graham, B.; Vas, G.; Wang, W.; Vermeylen, R.; Pashynska, V.; Cafmeyer, J.; Guyon, P.; Andreae, M. O.; Artaxo, P.; et al. Formation of Secondary Organic Aerosols Through Photooxidation of Isoprene. *Science* **2004**, *303*, 1173−1176.
(86) Wiegel, A. A.; Wilson, K. R.; Hinsberg, W. D.; Houle, F. A. Stochastic Methods for Aerosol Chemistry: a Compact Molecular Description of Functionalization and Fragmentation in the Heterogeneous Oxidation of Squalane Aerosol by OH Radicals. *Phys. Chem. Chem. Phys.* **2015**, *17*, 4398−4411.
(87) Nah, T.; Zhang, H.; Worton, D. R.; Ruehl, C. R.; Kirk, B. B.; Goldstein, A. H.; Leone, S. R.; Wilson, K. R. Isomeric Product Detection in the Heterogeneous Reaction of Hydroxyl Radicals with Aerosol Composed of Branched and Linear Unsaturated Organic Molecules. *J. Phys. Chem. A* **2014**, *118*, 11555−11571.
(88) Houle, F. A.; Hinsberg, W. D.; Wilson, K. R. Oxidation of a Model Alkane Aerosol by OH Radical: the Emergent Nature of Reactive Uptake. *Phys. Chem. Chem. Phys.* **2015**, *17*, 4412−4423.
(89) Wilson, K. R.; Smith, J. D.; Kessler, S. H.; Kroll, J. H. The Statistical Evolution of Multiple Generations of Oxidation Products in the Photochemical Aging of Chemically Reduced Organic Aerosol. *Phys. Chem. Chem. Phys.* **2012**, *14*, 1468.
(90) Koop, T.; Bookhold, J.; Shiraiwa, M.; Pöschl, U. Glass Transition and Phase State of Organic Compounds: Dependency on

DOI: 10.1021/acs.jpca.5b06946
J. Phys. Chem. A 2015, 119, 10767−10783

Molecular Properties and Implications for Secondary Organic Aerosols in the Atmosphere. *Phys. Chem. Chem. Phys.* **2011**, *13*, 19238.
(91) Arangio, A. M.; Slade, J. H.; Berkemeier, T.; Pöschl, U.; Knopf, D. A.; Shiraiwa, M. Multiphase Chemical Kinetics of OH Radical Uptake by Molecular Organic Markers of Biomass Burning Aerosols: Humidity and Temperature Dependence, Surface Reaction, and Bulk Diffusion. *J. Phys. Chem. A* **2015**, *119*, 4533−4544.
(92) Crounse, J. D.; Nielsen, L. B.; Jørgensen, S.; Kjaergaard, H. G.; Wennberg, P. O. Autoxidation of Organic Compounds in the Atmosphere. *J. Phys. Chem. Lett.* **2013**, *4*, 3513−3520.
(93) Mang, S. A.; Henricksen, D. K.; Bateman, A. P.; Andersen, M. P. S.; Blake, D. R.; Nizkorodov, S. A. Contribution of Carbonyl Photochemistry to Aging of Atmospheric Secondary Organic Aerosol. *J. Phys. Chem. A* **2008**, *112*, 8337−8344.
(94) Walser, M. L.; Park, J.; Gomez, A. L.; Russell, A. R.; Nizkorodov, S. A. Photochemical Aging of Secondary Organic Aerosol Particles Generated From the Oxidation of d-Limonene. *J. Phys. Chem. A* **2007**, *111*, 1907−1913.
(95) Epstein, S. A.; Blair, S. L.; Nizkorodov, S. A. Direct Photolysis of α-Pinene Ozonolysis Secondary Organic Aerosol: Effect on Particle Mass and Peroxide Content. *Environ. Sci. Technol.* **2014**, *48*, 11251−11258.
(96) Wong, J. P. S.; Zhou, S.; Abbatt, J. P. D. Changes in Secondary Organic Aerosol Composition and Mass Due to Photolysis: Relative Humidity Dependence. *J. Phys. Chem. A* **2015**, *119*, 4309−4316.
(97) Daumit, K. E.; Carrasquillo, A. J.; Hunter, J. F.; Kroll, J. H. Laboratory Studies of the Aqueous-Phase Oxidation of Polyols: Submicron Particles vs. Bulk Aqueous Solution. *Atmos. Chem. Phys.* **2014**, *14*, 10773−10784.
(98) Kwan, A. J.; Crounse, J. D.; Clarke, A. D.; Shinozuka, Y.; Anderson, B. E.; Crawford, J. H.; Avery, M. A.; McNaughton, C. S.; Brune, W. H.; Singh, H. B.; Wennberg, P. O.; et al. On the Flux of Oxygenated Volatile Organic Compounds From Organic Aerosol Oxidation. *Geophys. Res. Lett.* **2006**, *33*, L15815.
(99) Murphy, D. M.; Cziczo, D. J.; Hudson, P. K.; Thomson, D. S. Carbonaceous Material in Aerosol Particles in the Lower Stratosphere and Tropopause Region. *J. Geophys. Res.* **2007**, *112*, D04203.
(100) Heald, C. L.; Ridley, D. A.; Kreidenweis, S. M.; Drury, E. E. Satellite Observations Cap the Atmospheric Organic Aerosol Budget. *Geophys. Res. Lett.* **2010**, *37*, L24808.
(101) Spracklen, D. V.; Jimenez, J. L.; Carslaw, K. S.; Worsnop, D. R.; Evans, M. J.; Mann, G. W.; Zhang, Q.; Canagaratna, M. R.; Allan, J.; Coe, H.; et al. Aerosol Mass Spectrometer Constraint on the Global Secondary Organic Aerosol Budget. *Atmos. Chem. Phys.* **2011**, *11*, 12109−12136.

DOI: 10.1021/acs.jpca.5b06946
J. Phys. Chem. A 2015, 119, 10767−10783